Cardiovascular-Respiratory HUT Model including Optimal Control and Comparison to LBNP models

Martin Fink and Jerry J. Batzel and Franz Kappel*

Abstract

This report discusses modeling efforts designed to study the phenomenon of orthostatic stress. Orthostatic stress refers to stress placed on the cardiovascular system when the body is in the upright position as compared to the supine position. This report introduces a model of the cardiovascular and respiratory system which is used to simulate orthostatic stress. The model consists of cardiovascular and respiratory components and includes cardiovascular auto-regulation, ventilation control, and the baroreflex loop. Instead of an explicit formula for calculating the control response (sympathetic and parasympathetic response) from the pressures and blood gases, we use an inherent optimized control. Steady state analysis is given and model simulation is compared to experimental data we have collected using head up tilt (HUT) experiments. The simulations fit the measured data well and represent reasonable physiological values.

This work has led us to examine and report on several issues relating to orthostatic stress experiments. The head up tilt experiment (where gravity creates extra pressure stress on the lower body) is to be distinguished from the lower body negative pressure (LBNP) experiment where the lower body is subject to reduced exterior air pressure thus effectively increasing the venous capacitance due to less counteracting outside pressure. Both tests create blood volume shift to the lower body but the two physiological conditions are not equivalent. Because of some confusion created by mixing HUT and LBNP in the modeling literature, we compare two modeling representations and show that one implementation represents LBNP better while the other represents HUT better. We will present extended analysis in a later paper.

*in collaboration with Prof. Schneditz and Prof. Rössler, Universität Graz

Contents

1 Physiology

1.1 General cardiovascular and respiratory system function

Cardiovascular subsystem

The cardiovascular system (CVS) can be divided into two main circuits: the pulmonary and the systemic circuit. These circuits can be subdivided into four main vascular circuit components: pulmonary arterial, pulmonary venous, systemic arterial and systemic venous. The pulmonary system circuit connects the heart with the lung compartment, while the systemic system connects the heart to the tissue compartments where metabolism takes place. The lungs and the tissue compartments act as resistances in the flow of blood. An intricate control system acts to vary blood flow between tissue and lungs so as to maintain appropriate levels of nutrients, carbon dioxide CO_2, and oxygen O_2. Figure 1 provides a block diagram representation of this system. State variables for the CVS consist mainly of vascular pressures P_{as}, P_{vs}, P_{ap}, and P_{vp} where P_{as} represents arterial systemic pressure and the other quantities are similarly defined. Respiratory state variables are partial pressures for CO_2, and oxygen O_2 in the lungs and tissues.

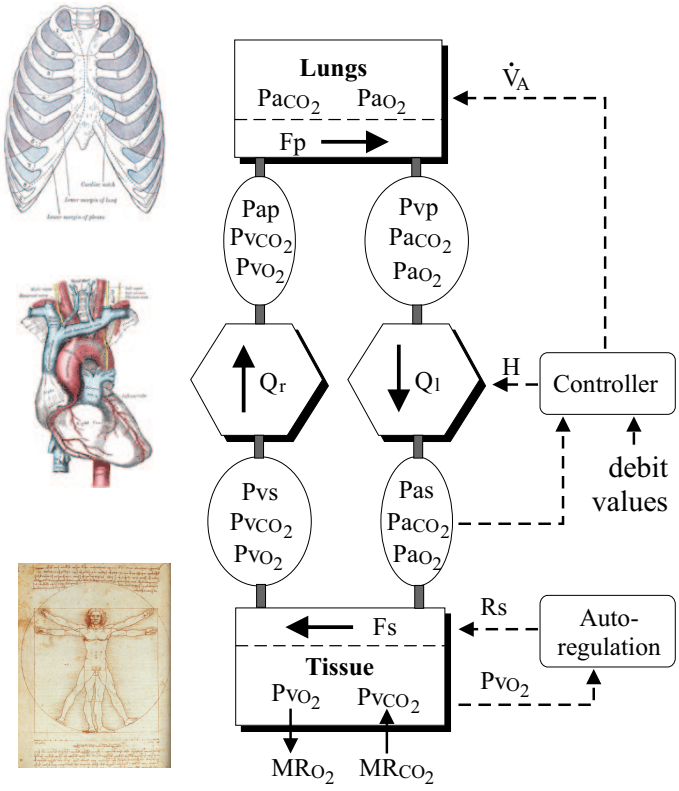

Figure 1: Basic CVS block diagram

A main function of the CVS control system is to maintain arterial blood pressure P_{as} at appropriate levels by varying cardiac output Q (via variation in heart rate H and heart contraction) and vascular systemic resistance and venous compliance. The steady state for various physiological conditions such as supine or standing is maintained by negative feedback loops which depend on sensing arterial and venous blood pressure at several sites. These steady states are most likely optimal for the system, although the nature of

this optimality is still debated. The short term control of P_{as} depends on global control mechanisms mediated by the sympathetic and parasympathetic nervous systems which modulate heart rate, contractility, systemic arterial resistance, and systemic venous compliance. There are also local control mechanisms for controlling vasodilation and resistance to insure that enough blood is delivered to organs when needed and which depend on local O_2 and CO_2 concentration. Longer term control mechanisms involve control of blood volume via the kidney and hormonal controls which also have other influences.

Respiratory subsystem

The respiratory system acts to exchange O_2 which is needed by the various tissues for metabolism for CO_2 which is produced by metabolic activity. Efficient exchange of these gases in the lungs depends on the ventilation rate $\dot{V}_A$ which is controlled by a negative feedback loop depending on sensors for CO_2 and O_2 located in the carotid artery and also sensors for brain tissue CO_2. A significant delay occurs in this feedback loop which can effect stability. This delay is caused by the time needed for the blood to transport these gases from the lungs to the sensory sites and hence this delay depends on Q. There are certain conditions where hypoxia can impact response to orthostatic stress which are not examined in this paper. In the tilt table experiment, which we will study, there is little deviation in blood gases and hence the transport delays are ignored.

The respiratory system in turn influences CVS resistance via oxygen concentration (brain and heart tissue also respond to CO_2 concentration) and there are also other mechanisms which act to match ventilation and cardiac output as well as synchronize respiratory and heart rate frequencies.

Modeling aspects, mass balance

These system components and their relation are depicted in Figure 1. Descriptions of blood flow depend on mass balance equations which are set up for the inflow and outflow of blood from these four main vascular compartments. Inflow comes from cardiac output Q while outflow denotes the blood flow (F) out of the vascular compartment and through the lung or tissue compartment considered as resistances. Auxiliary equations relating pressure, flow and resistance are essentially the same as Ohm's law. The following equations describe these flows for the arterial systemic, venous systemic, and venous pulmonary circuits.

$$\begin{aligned} c_{as}\dot{P}_{as}(t) &= Q_l(t) - F_s(t), \\ c_{vs}\dot{P}_{vs}(t) &= F_s(t) - Q_r(t), \\ c_{vp}\dot{P}_{vp}(t) &= F_p(t) - Q_l(t), \end{aligned}$$

Pulmonary arterial pressure P_{ap} is derived utilizing the assumption of fixed total blood volume V_0.

$$P_{ap}(t) = \frac{1}{c_{ap}}\Big(V_0 - c_{as}P_{as}(t) - c_{vs}P_{vs}(t) - c_{vp}P_{vp}(t)\Big).$$

The respiratory equations are developed in a similar way. Mass balance equations are set up for the inflow and outflow of CO_2 and O_2 from the lung and tissue compartments as transported by the pulmonary blood flow F_p and systemic tissue blood flow F_s. Ventilation $\dot{V}_A$ exchanges these gases in the lungs and metabolic rates MR create the opposite exchange in the tissue compartment.

$$
\begin{aligned}
V_{A_{CO_2}}\dot{P}_{a_{CO_2}}(t) &= 863F_p(t)\left(C_{v_{CO_2}}(t-\tau_V)-C_{a_{CO_2}}(t)\right)\\
&\quad +\dot{V}_A(t)\left(P_{I_{CO_2}}-P_{a_{CO_2}}(t)\right),\\
V_{A_{O_2}}\dot{P}_{a_{O_2}}(t) &= 863F_p(t)\left(C_{v_{O_2}}(t-\tau_V)-C_{a_{O_2}}(t)\right)\\
&\quad +\dot{V}_A(t)\left(P_{I_{O_2}}-P_{a_{O_2}}(t)\right),\\
V_{T_{CO_2}}\dot{C}_{v_{CO_2}}(t) &= MR_{CO_2}+F_s(t)\left(C_{a_{CO_2}}(t-\tau_T)-C_{v_{CO_2}}(t)\right),\\
V_{T_{O_2}}\dot{C}_{v_{O_2}}(t) &= -MR_{O_2}+F_s(t)\left(C_{a_{O_2}}(t)-C_{v_{O_2}}(t-\tau_T)\right),\\
V_{B_{CO_2}}\dot{C}_{B_{CO_2}}(t) &= MR_{B_{CO_2}}+F_B(t)\left(C_{a_{CO_2}}(t-\tau_B)-C_{B_{CO_2}}(t)\right),
\end{aligned}
$$

Section A in the appendix contains all symbol definitions. Control issues will be further discussed in Section 2 where the full model is described.

1.2 Orthostatic stress

Orthostatic stress refers to the stress induced on the cardiovascular system due to gravitational effects produced in the upright position as compared to the supine position. The main gravitational effect is the pooling of blood in the compliant venous compartment of + the lower body. This induces a fall in blood pressure which must be counteracted by the baroreflex which senses this drop. Heart rate and contractility are increased to raise the blood pressure and sympathetic activity responds by decreasing the capacitance in the venous compartment and also influences systemic resistance. The net result is that, while there is a shift of about 500 ml of blood to the venous compartment, mean arterial blood pressure remains unchanged while heart rate H is increased. The overall short term response depends on a combination of physiological reactions which may vary greatly between individuals. In some individuals, blood pressure is maintained by a large increase in contractility, small increase in H, and decrease in venous capacitance while in other individuals other combinations of change in H, contractility, and venous capacitance can occur.

Figure 2 illustrates the tilt table test which is used to study the effect of orthostatic stress. This effect takes on medical significance in those individuals who have inadequate transient response to orthostatic stress (such as the elderly) and in astronauts who exhibit orthostatic intolerance upon return to normal gravity.

According to the *Textbook of Physiology* (TP) [Pat89] the change in arterial resistance can be quite significant as sympathetic activity increases. As sympathetic activity increases from 0 to 10 Hz, the resistance increases up to 100 times for cutaneous arteries, 10 times in muscle and 5 times in renal arteries (p. 857 TP).

To see the impact of the gravitational force on blood pressure, note that transmural pressure increases in the feet from 98 mmHg in supine position to 198 mmHg in upright position. The difference of 100 mmHg equals a blood column of 130 cm (p. 776 TP). As mentioned above, the result is an increase in venous blood volume in upright position of 500 ml (p. 881 TP) as compared to the supine position. On the other hand Rowell [Row86] mentions a shift of 500–700 ml to the lower limbs and 200–300 ml to the pelvic region.

Among other orthostatic changes which occur between the supine and standing positions, there is general agreement that:

- venous capacitance decreases in upright position.
- Q decreases in upright position.
- H is generally higher in upright position.

- central venous pressure CVP is higher in supine position.
- stroke volume V_{Str} is higher in the supine position.

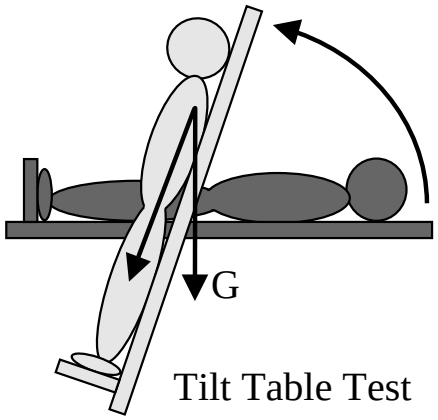

Figure 2: Orthostatic stress diagram

Figure 3 represents a system block diagram which introduces a division of the systemic vascular system into upper and lower systemic compartments and should be compared with Figure 1. Using this division, it is possible to distinguish between the upper and lower body and describe the influence of orthostatic stress and gravitational pressure on the lower compartment.

1.3 Control loops

Control loops are shown in block diagram Figure 3 for the respiratory and cardiovascular systems and represent the short term control response to perturbations in the steady state of the system. System control depends on sensory mechanisms which monitor critical state variables and respond to changes in these variables via negative feedback loops. The two main short term system loops represented in the diagram and which will be implemented in the model consist of the baroreflex loop which stabilizes arterial blood pressure and the respiratory control loop which controls levels of CO_2 (and indirectly pH) and O_2.

The baroreflex depends on arterial blood pressure sensors in the carotid and aortic bodies. These sensors send signals to the central control in the brain which responds via the sympathetic and parasympathetic systems to vary H, contractility, systemic resistance R, and venous compliance all of which influence arterial blood pressure P_{as}. There are also cardiopulmonary sensors (low pressure sensors) which respond to pressure changes in the right atrium and pulmonary arteries.

Another important control loop consists of the local autoregulation of tissue vascular resistance which responds to concentrations of O_2 (and in some cases CO_2 as well). This response reflects the changing needs of the tissues due to metabolic activity. The effect of O_2 concentration on vasodilation in muscle tissue is important for overall systemic resistance.

The respiratory peripheral chemosensors located in the carotid bodies respond to CO_2 and O_2 while the central chemosensors in the brain responds to CO_2. These sensors send information to the the central control processor in the medulla which varies the ventilatory rate V_A.

Implementation of the control processes which are represented in Figure 3 will be discussed in the next section.

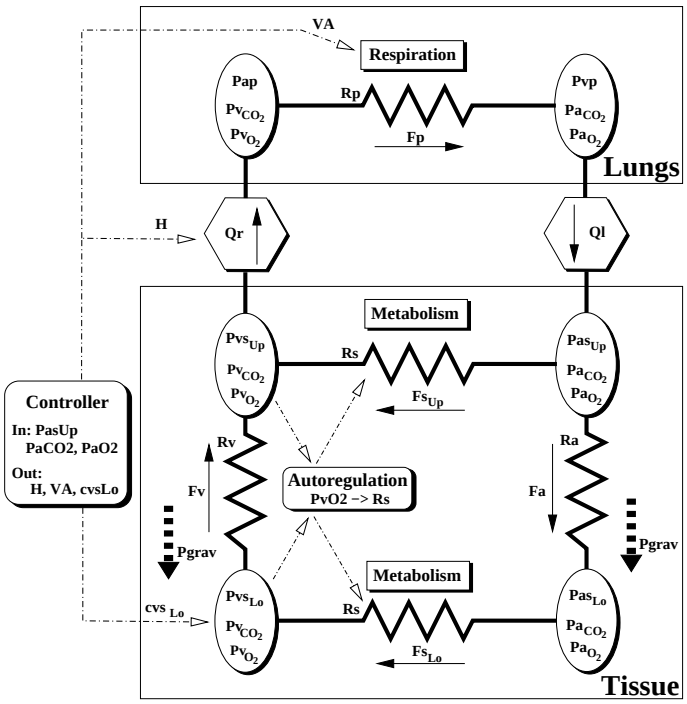

Figure 3: Orthostatic model block diagram

2 Orthostatic stress model

In this section we present the model equations which will be used to study orthostatic stress. The equations are adapted from earlier work of Kappel and Peer [Kap93] and Timischl [Tim98]. The model is augmented by two lower systemic vascular compartments where gravitation effects are introduced. The model consists of a set of nonlinear ordinary differential equations, auxiliary equations, and an optimal control mechanism. Model equations refer to states represented in block diagram Figure 3. Comparison of this Figure with Figure 1 shows how the original model has been adapted. There are now six vascular compartments and two respiratory compartments.

2.1 The basic ODEs

The basic model differential equations represent mass balance equations for blood flow (Eq. 2.1 to Eq. 2.5) and mass balance for blood gases (Eq. 2.6 to Eq. 2.10) as discussed in the last section. Equations 2.11 to 2.14 represent a model for contractility as influenced by H (Bowditch effect) while Equations 2.15 to 2.17 represent the control.

$$c_{asUp}\dot{P}_{asUp} = Q_l - F_a - F_{sUp} \tag{2.1}$$
$$c_{asLo}\dot{P}_{asLo} = F_a - F_{sLo} \tag{2.2}$$
$$c_{vsLo}\dot{P}_{vsLo} = F_{sLo} - F_v - \dot{c}_{vsLo}P_{vsLo} \tag{2.3}$$
$$c_{vsUp}\dot{P}_{vsUp} = F_v - Q_r + F_{sUp} \tag{2.4}$$
$$c_{vp}\dot{P}_{vp} = F_p - Q_l \tag{2.5}$$
$$V_{A_{CO_2}}\dot{P}_{a_{CO_2}} = 863F_p\left(C_{v_{CO_2}} - C_{a_{CO_2}}\right) + \dot{V}_A\left(P_{I_{CO_2}} - P_{a_{CO_2}}\right) \tag{2.6}$$
$$V_{A_{O_2}}\dot{P}_{a_{O_2}} = 863F_p\left(C_{v_{O_2}} - C_{a_{O_2}}\right) + \dot{V}_A\left(P_{I_{O_2}} - P_{a_{O_2}}\right) \tag{2.7}$$
$$V_{B_{CO_2}}\dot{C}_{B_{CO_2}} = MR_{B_{CO_2}} + F_B\left(C_{a_{CO_2}} - C_{B_{CO_2}}\right) \tag{2.8}$$
$$V_{T_{CO_2}}\dot{C}_{v_{CO_2}} = MR_{CO_2} + F_s\left(C_{a_{CO_2}} - C_{v_{CO_2}}\right) \tag{2.9}$$
$$V_{T_{O_2}}\dot{C}_{v_{O_2}} = -MR_{O_2} + F_s\left(C_{a_{O_2}} - C_{v_{O_2}}\right) \tag{2.10}$$
$$\dot{S}_l = \sigma_l \tag{2.11}$$
$$\dot{S}_r = \sigma_r \tag{2.12}$$
$$\dot{\sigma}_l = -\gamma_l\sigma_l - \alpha_l S_l + \beta_l H \tag{2.13}$$
$$\dot{\sigma}_r = -\gamma_r\sigma_r - \alpha_r S_r + \beta_r H \tag{2.14}$$
$$\dot{H} = u_1 \tag{2.15}$$
$$\ddot{V}_A = u_2 \tag{2.16}$$
$$\dot{c}_{vsLo} = u_3. \tag{2.17}$$

Section A in the appendix contains all symbol definitions. Control issues will be further discussed below in Section 2.5.

2.2 Cardiovascular auxiliary equations

The first auxiliary cardiovascular equation (Eq. 2.18) describes pulmonary arterial pressure in terms of the other cardiovascular pressures. Equations 2.19 and 2.20 describe relations for Q in terms of stroke volume, preload and afterload (see [Kap93] for details). Equation 2.21 implements a maximum condition so that stroke volume does not exceed the filling volume. Equation 2.22 describes the time of diastole in terms of H.

$$P_{ap}(t) = \frac{1}{c_{ap}}\Big(V_0 - c_{asUp}P_{asUp}(t) - c_{asLo}P_{asLo}(t) - c_{vsUp}P_{vsUp}(t) - c_{vsLo}(t)P_{vsLo}(t) - c_{vp}P_{vp}(t)\Big). \quad (2.18)$$

$$Q_l(t) = H\frac{c_l P_{vp}(t) f\Big(S_l(t), P_{asUp}(t)\Big)\Big(1 - e^{-t_d/(R_l c_l)}\Big)}{P_{asUp}(t)\Big(1 - e^{-t_d/(R_l c_l)}\Big) + f\Big(S_l(t), P_{asUp}(t)\Big)e^{-t_d/(R_l c_l)}}, \quad (2.19)$$

$$Q_r(t) = H\frac{c_r P_{vsUp}(t) f\Big(S_r(t), P_{ap}(t)\Big)\Big(1 - e^{-t_d/(R_r c_r)}\Big)}{P_{ap}(t)\Big(1 - e^{-t_d/(R_r c_r)}\Big) + f\Big(S_r(t), P_{ap}(t)\Big)e^{-t_d/(R_r c_r)}}. \quad (2.20)$$

$$f(s,p) = 0.5(s+p) - 0.5\left((p-s)^2 + 0.01\right)^{1/2} \quad (2.21)$$

$$t_d = \frac{60}{H} - \kappa\left(\frac{60}{H}\right)^{1/2}, \quad (2.22)$$

2.3 Respiratory auxiliary equations

Auxiliary equations for the respiratory system consist of an equation for cerebral blood flow (Eq. 2.23), and dissociation equations (Eq. 2.24 to Eq. 2.28) relating partial pressures and concentrations of blood gases. Equation 2.29 represents a physiological formula for minute ventilation to be used for reference. Minute ventilation ($\dot{V}_E$) is the air actually entering or leaving the body and is to be distinguished from alveolar ventilation $\dot{V}_A$ which is the volume of air actually involved in exchange of blood gases in the alveoli (and in some of the small airways). The difference (see Eq. 2.30) is the dead space volume $\dot{V}_D$ which represents the volume of air within the larger conducting tubes of the lungs which do not exchange gases with blood. We will model $\dot{V}_A$ using an optimal control approach (See Subsection 2.5).

$$F_B(t) = F_{B_0}\left(1 + 0.03\left(P_{a_{CO_2}}(t) - 40\right)\right). \quad (2.23)$$

$$C_{a_{O_2}}(t) = K_1\left(1 - e^{-K_2 P_{a_{O_2}}(t)}\right)^2, \quad (2.24)$$

$$C_{v_{O_2}}(t) = K_1\left(1 - e^{-K_2 P_{v_{O_2}}(t)}\right)^2, \quad (2.25)$$

$$C_{a_{CO_2}}(t) = K_{CO_2}P_{a_{CO_2}}(t) + k_{CO_2}, \quad (2.26)$$

$$C_{v_{CO_2}}(t) = K_{CO_2}P_{v_{CO_2}}(t) + k_{CO_2}, \quad (2.27)$$

$$C_{B_{CO_2}}(t) = K_{CO_2}P_{B_{CO_2}}(t) + k_{CO_2}. \quad (2.28)$$

$$\dot{V}_E = G_p e^{-0.05P_{a_{O_2}}}\left(P_{a_{CO_2}} - I_p\right) + G_c\left(P_{a_{CO_2}} - I_c\right), \quad (2.29)$$

$$\dot{V}_A = \dot{V}_E - \dot{V}_D. \quad (2.30)$$

2.4 The flows

The inter-compartment blood flows are defined by

$$F_v = \max\big(0; P_{vsLo} - P_{vsUp} - P_{grav}\big)/R_v \tag{2.31}$$
$$F_a = \left(P_{asUp} - P_{asLo} + P_{grav}\right)/R_a \tag{2.32}$$
$$F_{sUp} = \left(P_{asUp} - P_{vsUp}\right)/R_s \tag{2.33}$$
$$F_{sLo} = \left(P_{asLo} - P_{vsLo}\right)/R_s \tag{2.34}$$
$$F_p = \left(P_{ap} - P_{vp}\right)/R_p \tag{2.35}$$

where the *max* function implements the action of the venous valves to avoid backflow. P_{grav} represents the hydrostatic pressure induced on the lower compartments. The derivation of this implementation will be discussed in Section 4.

Also

$$R_s = A_{pesk} P_{v_{O_2}} \tag{2.36}$$
$$F_s = F_{sUp} + F_{sLo} \tag{2.37}$$
$$P_{grav} = c\rho g h \sin(TiltingAngle) \tag{2.38}$$

where $\rho = 1.05$ mg/mm^3 $= 1050$ kg/m^3 and $c = 1/133.322$ mmHg/Pa. Eq. 2.36 describes the effect of oxygen concentration on systemic resistance. Mechanisms which act to match ventilation and cardiac output as well as synchronize respiratory and heart rate frequencies are ignored. Eq. 2.37 describes the flow through the tisue compartment. Eq. 2.38 describes the dependency of the gravitation effect on the degree of tilt.

2.5 The optimal control

The control functions u_1, u_2, and u_3 represent the variations in heart rate H, ventilation rate $\dot{V}_A$, and venous capacitance c_{vsLo}. The control of venous capacitance includes the baroreflex and may reflect the nonlinearity in the pressure-volume relation. There is disagreement over the degree to which the change in capacitance is active or passive (e.g. [Ste01]), which can be reflected by the weights of the control. Changes in systemic resistance and contractility are modeled via parameter changes.

We model the control action as an optimal control via a cost functional. The transition from an initial (steady state) disturbance to the final steady state is optimal in the sense that controlled values P_{as}, P_{vs}, $P_{a_{CO_2}}$, and $P_{a_{O_2}}$ are stabilized such that deviations from their final steady state values are as small as possible. Furthermore, H, $\dot{V}_A$, and c_{vsLo} are prevented from changing too fast or too extensively.

The stationary equations for the system (Eq. 2.1) to (Eq. 2.17) determine a two-parameter set of steady states. Therefore we need to choose the steady state values of two state variables as parameters. In general we choose values for $P_{a_{CO_2}}$ and H.

Mathematically, this can be formulated in the following way. To transfer the system to the final or target steady state, we determine control functions such that the cost functional

$$\int_0^\infty q_a \left(P_{asUp} - P^f_{asUp}\right)^2 + q_v \left(P_{vsUp} - P^f_{vsUp}\right)^2 + q_{CO} \left(P_{a_{CO_2}} - P^f_{a_{CO_2}}\right)^2 + q_O \left(P_{a_{O_2}} - P^f_{a_{O_2}}\right)^2 + q_1 \left(u_1\right)^2 + q_2 \left(u_2\right)^2 + q_3 \left(u_3\right)^2 \, dt \tag{2.39}$$

is minimized under the restriction

$$\dot{x}(t) = g\big(x(t)\big) + B\, u(t), \qquad x(0) = x^i. \tag{2.40}$$

The values q_i are weights defining the degree of influence of quantities on the cost. q_a represents the influence of the arterial baroreceptor loop and q_v the influence of the cardio-pulmonary baroreceptor loop.

In modeling the transition from the initial "resting supine" steady state to the final "head up tilt" state the following steps are carried out:

- Compute the steady states "resting supine", x^s, and "head up tilt", x^h.
  Here the steady state "head up tilt" is defined by parameter changes:
  - P_{grav} increased based on the degree of tilt and Eq. 2.38,
  - higher heart rate H,
  - lowered capacitance, higher resistance, and increase contractility.
- The control functions u_1, u_2, and u_3 which transfer the system (Eq. 2.1 to Eq. 2.17) from the initial steady state "supine", x^s, to the final steady state "head up tilt", x^h, are found as follows. We consider the linearized system around x^h with initial condition $x(0) = x^s$, and the cost functional (2.39).

$$\int_0^\infty q_a\left(P_{asUp} - P^h_{asUp}\right)^2 + q_v\left(P_{vsUp} - P^h_{vsUp}\right)^2 + q_{CO}\left(P_{a_{CO_2}} - P^h_{a_{CO_2}}\right)^2 + q_O\left(P_{a_{O_2}} - P^h_{a_{O_2}}\right)^2 + q_1\left(u_1\right)^2 + q_2\left(u_2\right)^2 + q_3\left(u_3\right)^2\, dt$$

  Here, superscript "s" and superscript "h" will refer to the steady state values "supine" and "head up tilt" respectively. These states are defined by parameter choices defining these states. We then compute the control functions u_1, u_2, and u_3 such that the cost functional is minimized subject to the linearized system. This is accomplished by solving an algebraic matrix-Riccati equation. In particular, u_1, u_2 and u_3 are given as feedback control functions.
- This control is used to stabilize the nonlinear system (2.1) to (2.17). This control will be suboptimal in the sense of Russell [Rus79].

We may implement step changes in P_{grav}, systemic resistance, and contractility, or introduce smooth changes over a short tilt time. In the later case, though the system is now nonautonomous, we still implement the control functions u_1, u_2, and u_3 calculated for a time-independent linear system around the final steady state "head up tilt". This further reduces the optimality but the thereby obtained (suboptimal) control still stabilizes the system and is useful for dynamic studies.

3 Modeling history

Several articles have been published, which describe models including orthostatic stress – either head up tilt (HUT) or lower body negative pressure (LBNP). See for instance [Boy72], [Cro74], [Leo79], [Whi83], [Mel92], [Sud93], [Kar94], [Mel94], [Bur00], [Pet02], [Wal01], [Hel02], and [Hao03].

LBNP modifies the impact internal blood pressure has on the volume V of a compartment by varying the transmural pressure P_{trans}. Even though some models change the compliance c, too.

$$V = f(c, P_{trans}), \quad P_{trans} = P - P_{LBNP} \tag{3.1}$$

HUT models most often change the blood flow q into, out of, or through the compartment according to the tilting angle Θ.

$$q = q^0 + G \sin \Theta \tag{3.2}$$

[Sud93] LBNP

$$q_i = (p_l - p_m) \times c_i$$

where p_l and p_m are pressures at beginning and end of tube, q_i is the flow through the i-th tube. Sud et al. approximated the compliance c_i by a polynomial of p_l, p_m, p_{ext} ($p_{ext} \hat{=} P_{LBNP}$).

[Mel94] LBNP

Melchior et al. consider deviations from 'normal'.

$$\Delta P_{trans} = \Delta CVP - K_{trans} P_{LBNP}$$
$$\Delta V = \frac{2V_m}{\pi} \arctan\left(\pi C_0 \frac{\Delta P_{trans}}{2V_m}\right)$$

The volume increments ΔV tend to 0 when ΔP_{trans} tends to 0, and they approach V_m for large values of ΔP_{trans}. (Blood shifts to lower limbs in HUT 500–700 ml and in pelvic region 200–300 ml according to a citation of Rowell)

By using a nonlinear compliance they include the effect of an unstressed volume.

[Wal01] HUT and LBNP

$$\frac{\partial A}{\partial t} + \frac{\partial (AU)}{\partial x} = 0$$
$$\frac{\partial U}{\partial t} + U \frac{\partial U}{\partial x} = -\frac{1}{\rho} \frac{\partial P_t}{\partial x} - FU - G \cos(\Theta)$$
$$P_t = P - P_e = K \, \Phi(A/A_0)$$

where P_e external pressure, P fluid pressure, A cross section (A_0 unstressed), U flow speed, ρ density, F friction, K stiffness, and $\Phi(\cdot)$ tube law. The LBNP is implemented modifying the transmural pressure P_t and gravity is changing the flow directly.

[Pet01] HUT

Peterson et al. don't give a single equation in this article, so it is difficult to tell how they implemented the pressure changes because of the gravity, but as they refer to hydrostatic pressure one may assume something similar as Walsh et al. and we did.

[Hel02] HUT and LBNP

$$\frac{d}{dt}\Big(c\,(P_n - P_{bias})\Big) = \frac{P_{n-1} - P_n}{R_n} - \frac{P_n - P_{n+1}}{R_{n+1}}$$

Heldt uses the same implementation for HUT and LBNP, what brought us to our considerations in Section 5. P_i are compartmental pressures and P_{bias} represents the orthostatic stress (either HUT or LBNP).

[Hao03] LBNP

The model of Hao et al. is directly derived from [Mel94]. The add on consists of the extension of the model for negative P_{trans} which leads to negative volume change and at last to collapse of the vessels (using the same equations with different parameters).

4 Derivation of orthostatic effects

There are different ways to view the action of the gravitational force on the system of blood vessels, which are discussed in this section.

In supine position the gravitational force is perpendicular to the body and thus doesn't have significant influence on the cardiovascular system and in particular the flows. When standing the direction of gravitation is parallel to the body and thus it acts on the blood cells in the direction of the arteries and veins. – The weight of the upper blood cells presses on the lower cells.

Hydrostatic theory shows, that the pressure occurring at a certain hight is independent of the form of the vessels above, it only depends on the height of the column, because all other forces are compensated by the vessel walls.

In our model we split the arterial and venous systemic compartments in an upper and a lower part, for distinction of vessels and tissue at about heart level and at a much lower level. The pressures at heart level (P_{asUp} and P_{vsUp}) are the pressures we always measure when visiting the doctor. These pressures act on the lower compartments and influence the flow into or out of them, and, as mentioned before, in tilt there is an additional pressure (here called P_{bias}), depending on the tilting angle, which comes from the weight of blood in the upper compartments acting on the lower ones.

In general the flow between two compartments is defined by Ohm's law

$$F = \frac{P_{in} - P_{out}}{R}.$$

Focusing for a moment only on the upper and lower compartments on the arterial side, the pressure-flow relationship would be given by

$$F_a = \frac{(P_{asUp} + P_{bias}) - P_{asLo}}{R_a}. \tag{4.1}$$

The pressures in this approach reflect the actual pressures inside the compartments, thus P_{asLo} is a combination of the dynamic pressure and the hydrostatic or tilting pressure (i.e. $P_{asLo} = P^{dyn}_{asLo} + P_{bias}$, but $P_{asUp} = P^{dyn}_{asUp}$).

Note that substituting the expression for P_{asLo} the hydrostatic and gravitational effects cancel.

Similarly on the venous side (including the maximum function representing the venous valves) we have

$$F_v = \frac{1}{R_a} \max\Big(0; P_{vsLo} - (P_{vsUp} + P_{bias})\Big) \tag{4.2}$$

and between the lower compartments we have the "normal" flow

$$F_{sLo} = \frac{P_{asLo} - P_{vsLo}}{R_s}. \tag{4.3}$$

Starting from the view that the kinetic energy and thus the flow is independent of hydrostatic effects (see Berne&Levy [Ber97] and Rowell [Row93]) we develop the following relation.

If the flow is given by just the dynamical pressures and noting that $P_{asLo} = P^{dyn}_{asLo} + P_{bias}$ and $P_{asUp} = P^{dyn}_{asUp}$, we derive that

$$F_a = \frac{P^{dyn}_{asUp} - P^{dyn}_{asLo}}{R_a} = \frac{P_{asUp} - (P_{asLo} - P_{bias})}{R_a} \tag{4.4}$$

$$F_v = \frac{1}{R_a} \max\Big(0; P^{dyn}_{vsLo} - P^{dyn}_{vsUp}\Big) = \frac{1}{R_a} \max\Big(0; (P_{vsLo} - P_{bias}) - P_{vsUp}\Big) \tag{4.5}$$

$$F_{sLo} = \frac{(P_{asLo} - P_{bias}) - (P_{vsLo} - P_{bias})}{R_s}, \tag{4.6}$$

which are equivalent to the flows given above.

Starting from the viewpoint of compartment volumes, V_{asLo} for example increases if there is more inflow than outflow and vice versa, that is

$$\frac{d\,V_{asLo}}{dt} = F_a - F_{sLo}. \tag{4.7}$$

The volume of a compartment is related to the overall pressure inside the compartment (hydrostatic plus dynamic). Simplified this function can be assumed to be linear.

$$V_{asLo} = c_{asLo}(P^{dyn}_{asLo} + P_{bias}) \tag{4.8}$$

Differentiating Eq. (4.8) and combining it with Eq. (4.7) we get

$$\begin{aligned} \frac{d}{dt}\Big(c_{asLo}(P^{dyn}_{asLo} + P_{bias})\Big) &= F_a - F_{sLo} \\ &= \frac{P_{asUp} - P^{dyn}_{asLo}}{R_a} - \frac{P^{dyn}_{asLo} - P^{dyn}_{vsLo}}{R_s} \end{aligned} \tag{4.9}$$

and similarly

$$\frac{d}{dt}\Big(c_{vsLo}(P^{dyn}_{vsLo} + P_{bias})\Big) = \frac{P^{dyn}_{asLo} - P^{dyn}_{vsLo}}{R_s} - \frac{P^{dyn}_{vsLo} - P_{vsUp}}{R_v}. \tag{4.10}$$

The hydrostatic pressure increases the volume of the lower compartments, which indirectly influences the flows and the dynamical pressures of the system, which all happens simultaneously.

To get the actual pressures (including the hydrostatic pressure) inside the compartments (e.q. $P_{asLo} = P^{dyn}_{asLo} + P_{bias}$), we plug in $P^{dyn}_{asLo} = P_{asLo} - P_{bias}$ and $P^{dyn}_{vsLo} = P_{vsLo} - P_{bias}$.

We find that

$$\frac{d}{dt}\Big(c_{asLo}P_{asLo}\Big) = \frac{P_{asUp} - (P_{asLo} - P_{bias})}{R_a} - \frac{(P_{asLo} - P_{bias}) - (P_{vsLo} - P_{bias})}{R_s}$$
$$\frac{d}{dt}\Big(c_{vsLo}P_{vsLo}\Big) = \frac{(P_{asLo} - P_{bias}) - (P_{vsLo} - P_{bias})}{R_s} - \frac{(P_{vsLo} - P_{bias}) - P_{vsUp}}{R_v}$$

which is again equivalent to the two approaches from before and our model equations:

$$\frac{d}{dt}\Big(c_{asLo}P_{asLo}\Big) = \frac{P_{asUp} - (P_{asLo} - P_{bias})}{R_a} - \frac{P_{asLo} - P_{vsLo}}{R_s} \tag{4.11}$$
$$\frac{d}{dt}\Big(c_{vsLo}P_{vsLo}\Big) = \frac{P_{asLo} - P_{vsLo}}{R_s} - \frac{(P_{vsLo} - P_{bias}) - P_{vsUp}}{R_v} \tag{4.12}$$

Note: Equations (4.9) and (4.10) can also be derived from the viewpoint of lower body negative pressure with P_{bias} the absolute value of the applied pressure (see [Hel02]).

5 Comparison of two models of orthostatic stress

As mentioned above, the head up tilt (HUT) experiment involves tilting a resting supine subject to varying degrees of head up orthostasis (in varying amounts of time) using a tilt table. Cardiovascular steady state and dynamic response are measured for various quantities. The stress is induced by gravitational effects on blood flow and distribution. Lower body negative pressure tests involve reducing the exterior air pressure on the lower torso which results in changing effective venous compliance.

There are a number of ways to implement the effects produced by these experiments depending on the different points of action on the system (see Section 3). There are examples in the literature of modeling efforts which use a single basic implementation to represent HUT and LBNP (e.g. [Hel02]). Furthermore, these two conditions are often treated as representing the same physiological situation. The degree to which one implementation can represent both cases has not been fully discussed in the literature.

To clarify these issues and find some conditions under which HUT and LBNP can be treated as the same effect and when it is necessary to make a distinction, we take a closer look at the modeling aspects by comparing two models, on which directly implements LBNP and the other implementing HUT.

5.1 LBNP model

As proposed in [Hel02], orthostatic stress is modeled by the variable P_{bias}, changing the external and thus transmural pressure and the pressure-volume characteristics. See Figure 4 LBNP case.

$$
\begin{aligned}
q_1 &= \left(P_{n-1} - P_n\right)/R_n \\
q_2 &= \left(P_n - P_{n+1}\right)/R_{n+1} \\
q_3 &= \frac{d}{dt}\Big(C_n\left(P_n - P_{bias}\right)\Big)
\end{aligned}
$$

This clearly models the LBNP case but does it also implement HUT with the same degree of physiological fidelity?

5.2 HUT model

For HUT we introduced in our model, the variable P_{grav} to model gravitational hydrostatic pressure, as discussed in Section 2, which changes the flow between compartments of different heights. See Figure 4 HUT case.

$$
\begin{aligned}
q_1 &= \left(P_{n-1} + P_{grav} - P_n\right)/R_n \\
q_2 &= \left(P_n - P_{n+1}\right)/R_{n+1} \\
q_3 &= \frac{d}{dt}\Big(C_n P_n\Big)
\end{aligned}
$$

5.3 Comparison

In this section we take a look at the steady state and the dynamic responses of the two models consisting of two (e.g. leg) compartments at the same height as represented in the two cases of Fig. 4. The application of lower body negative pressure stress and tilt stress will be referred to as orthostatic stress.

We keep the pressures at the inflow and outflow of the system constant to get a clearer picture of the orthostatic effects, which may be done in experiments with animals, too.

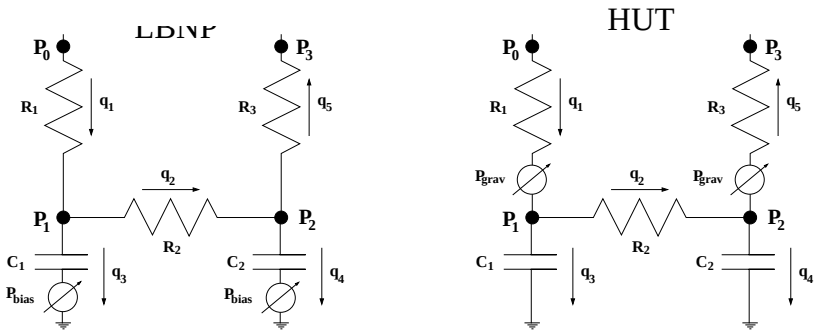

Figure 4: The structures of two compartment models: LBNP (left) and HUT (right)

For the simulations we use ramp functions for P_{bias} and P_{grav} where $P_{bias} = -P_{grav}$. The pressure at the inflow P_0 is held constant for the simulations, the first compartment is represented by P_1 (arterial compartment), the second by P_2 (venous compartment) and pressure P_3 is held constant again.

The equations representing the two cases in Fig. 4 are given as:

LBNP model

$$\frac{d(c_1 P_1)}{dt} = \frac{d(c_1 P_{bias})}{dt} + \frac{P_0 - P_1}{R_1} - \frac{P_1 - P_2}{R_2} \tag{5.1}$$

$$\frac{d(c_2 P_2)}{dt} = \frac{d(c_2 P_{bias})}{dt} + \frac{P_1 - P_2}{R_2} - \frac{P_2 - P_3}{R_3} \tag{5.2}$$

HUT model

$$\frac{d(c_1 P_1)}{dt} = \frac{P_{grav}}{R_1} + \frac{P_0 - P_1}{R_1} - \frac{P_1 - P_2}{R_2} \tag{5.3}$$

$$\frac{d(c_2 P_2)}{dt} = \frac{P_{grav}}{R_3} + \frac{P_1 - P_2}{R_2} - \frac{P_2 - P_3}{R_3} \tag{5.4}$$

5.3.1 Steady states

The steady states are easy to calculate:

LBNP model

$$P_1 = \frac{P_0(R_2 + R_3) + P_3 R_1}{R_1 + R_2 + R_3}$$

$$P_2 = \frac{P_0 R_3 + P_3(R_1 + R_2)}{R_1 + R_2 + R_3}$$

HUT model

$$P_1 = \frac{P_0(R_2 + R_3) + P_3 R_1}{R_1 + R_2 + R_3} + P_{grav}$$

$$P_2 = \frac{P_0 R_3 + P_3(R_1 + R_2)}{R_1 + R_2 + R_3} + P_{grav}$$

The steady state of the LBNP model is independent of the degree of induced orthostatic stress, which is reasonable for LBNP, but surely not for HUT. At application of LBNP the pressure may decrease for a short while, but afterwards will be maintained at the same level as the initial steady state (as long as the inflow and outflow pressures are

kept constant). In HUT the hydrostatic pressure change due to gravity must be added to the normal (supine) pressure, which is reflected in the HUT equations, but not in the LBNP model.

So the pressure steady states are not identical for HUT and LBNP, but according to the models the steady state flows through the compartments are the same

$$q = \frac{P_0 - P_3}{R_1 + R_2 + R_3}$$

which shows, that the steady state flows are independent of the way that orthostatic stress is induced (treatment) – as long as inflow and outflow pressures are kept constant.

Also the steady state volumes in the compartments are the same

$$V_1^L = c_1(P_1^L - P_{bias}) = c_1(P_1^L + P_{grav}) = c_1\left(\frac{P_0(R_2+R_3) + P_3R_1}{R_1+R_2+R_3} + P_{grav}\right) = c_1P_1^H = V_1^H$$

$$V_2^L = c_2(P_2^L - P_{bias}) = c_2(P_2^L + P_{grav}) = c_2\left(\frac{P_0R_3 + P_3(R_1+R_2)}{R_1+R_2+R_3} + P_{grav}\right) = c_2P_2^H = V_2^H$$

Conclusion: The two models have different predictions for the compartment internal pressures, but agree on flow and volume predictions for steady state. Viewed from the outside (as black boxes) the flow behaviors in steady state are indistinguishable, even though internal pressures are different.

5.3.2 Simulations

Fig. 5 shows that both models have different pressure dynamics for the two compartments. The pressures P_1 and P_2 (in Fig. 4) act like arterial and venous pressures because of the choices we make for the two compliance values ($c_1 = 0.01$, $c_2 = 0.643$) and for the input and output pressures ($P_0 = 90$, $P_3 = 10$).

$P_{grav} = -P_{bias}$ goes from 0 to 50 mmHg and the resistances are set to $R_1 = 0.01$, $R_2 = 15$, $R_3 = 0.01$.

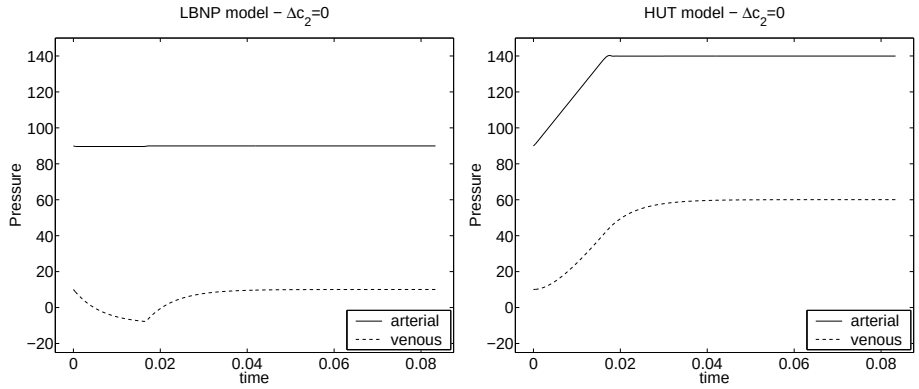

Figure 5: Left: LBNP model pressure dynamics, right: HUT model pressure dynamics.

From physiology we expect, that in HUT the pressure in the lower parts increases to a certain steady state – which is represented by HUT model.

The LBNP model shows different effects, which can be explained by taking a closer look at the equations. – If we look again at the steady states before tilt and after tilt, we notice that they are the same because $\frac{d}{dt}P_{bias} = 0$ in both cases and thus the value of P_{bias} is not relevant for the steady states. This is reasonable for LBNP, because the

whole body is at one level – so after applying the LBNP the compartments have to return to the same pressure steady states (assuming we keep the inflow and outflow pressures constant).

The internal pressure dynamics are different for the two cases.

When we look at the net inflow (difference of inflow and outflow) for the two models and for each compartment, we get graphs as in Fig. 6.

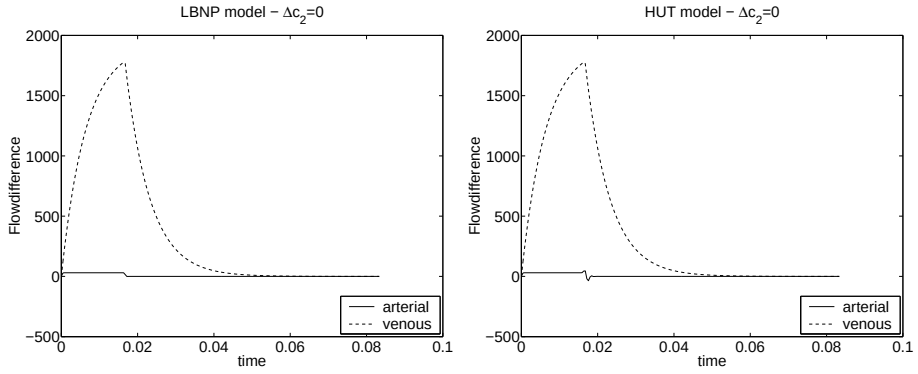

Figure 6: Net inflow into each compartment. Left: LBNP model, right: HUT model.

We choose $P_{bias} < 0$ to get similar results as in HUT, leading to the results shown here. Note that in the paper [Hel02] it seems that Heldt chose $P_{bias} > 0$, so the flow characteristic would be reversed and the compartment would push blood into the circulation instead of pulling it out. This appears to be a typographical error.

The dynamics of the net flows in Fig. 6 look identical, which is surprising given the apparent difference in the model equations.

From Fig. 7 which represents the difference between the flows of the two models, we see that the simulations do not give quite the same results, but the question is, whether this is a numerical artifact or represents a real difference in the predictions of the models.

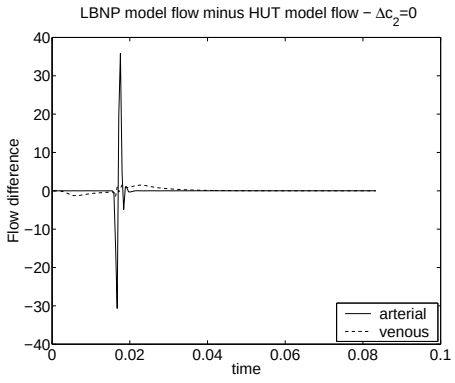

Figure 7: Difference in flows between LBNP and HUT

Since the capacitance plays an important role in orthostatic stress, we next examine the effect of variable capacitance on the behavior of the two models.

In the following figures venous compliance c_2 changes via a ramp function. Δc represents the maximum change in the capacitance.

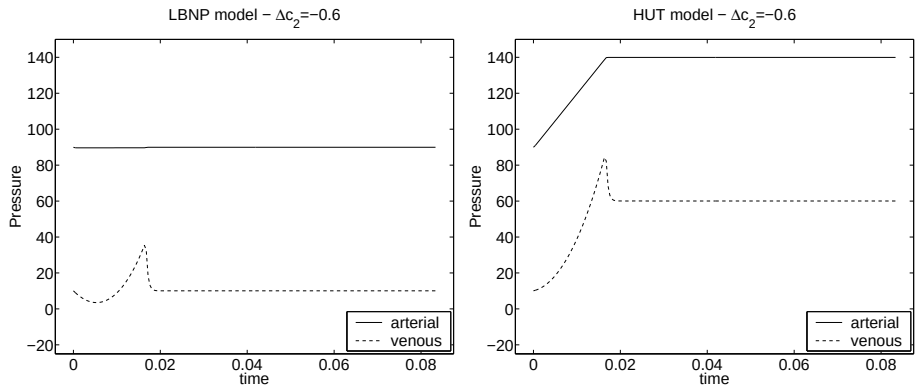

Figure 8: Pressure dynamics in the compartments including capacitance change. Left: LBNP model, right: HUT model.

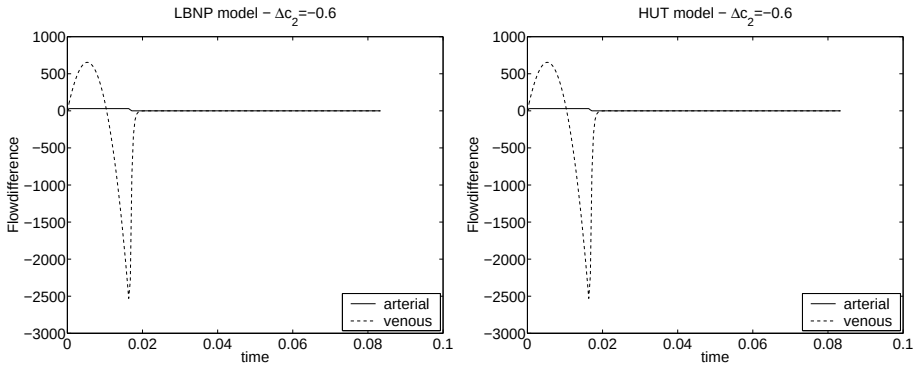

Figure 9: Net inflow into each compartment including capacitance change. Left: LBNP model, right: HUT model.

Once again we see that the pressure dynamics (Fig. 8) are different between the models. However, there again appears to be no significant difference in the net flows (Fig. 9).

Fig. 10 exhibits the difference between model flows with variable capacitance. It is clear that the difference in behavior is greater than with fixed capacitance, but still quite small.

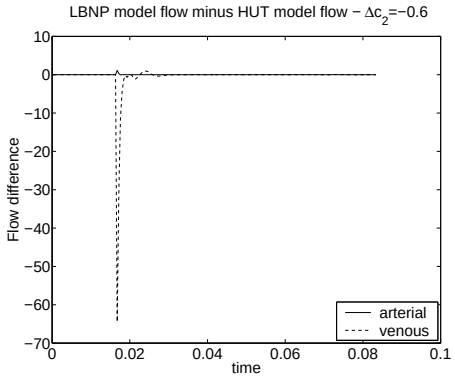

Figure 10: Difference in flows between LBNP and HUT including variable capacitance

5.3.3 Analytical results

In Section 4 we alluded to the fact, that the equations incorporating lower body negative pressure can be transformed into equations representing orthostatic stress with hydrostatic pressure.

The difference in the two-dimensional models discussed here is represented by transformations in the pressure representations. Thus an implementation with a negative external pressure implies a compartment pressure different from what is expected from an additional hydrostatic component to the compartment pressure.

The transformation of Equations (4.9 and 4.10) to Equations (4.11 and 4.12) is equivalent to the transformation of Equations (5.1 and 5.2) to Equations (5.3 and 5.4).

The transformations are accomplished by substitutions using the following equivalences:

$$P_1^{HUT} = P_1^{LBNP} + P_{bias} \qquad P_2^{HUT} = P_2^{LBNP} + P_{bias}. \tag{5.5}$$

Using the transformations above, the flows can be shown to be equivalent. For instance

$$\begin{aligned} q_1^{HUT} &= \frac{P_0 + P_{bias} - P_1^{HUT}}{R_1} \\ &= \frac{P_0 + P_{bias} - P_1^{HUT}}{R_1} \\ &= \frac{P_0 + P_{bias} - (P_1^{LBNP} + P_{bias})}{R_1} \\ &= \frac{P_0 - P_1^{LBNP}}{R_1} \\ &= q_1^{LBNP}. \end{aligned}$$

Conclusion: The following points summarize these results:

- The internal lower body pressures differ very much between models as between LBNP and HUT.
- The dynamic flows are the same for both models. The differences in the simulations represent numerical artifacts.
- These LBNP and HUT models are indistinguishable when only considering upper body pressures, which illustrates the basis for using LBNP as an approximation of HUT when restricted to certain physiological measurements.
- The actual pressures in the lower body can only be modeled using the associated model. For modeling experiments with LBNP and HUT the model must consist of both representations.
- There may be a difference of the controls of venous capacitance $c_2(t)$ between LBNP and HUT, which was not addressed yet.

6 Steady state analysis

At steady state there are no changes in time, thus the right-hand sides of the model ODEs are equal to zero. So we can solve for the flows and for the state variables.

6.1 The flows at steady state

The following flow relations are given:

$$F_a = F_{sLo} = F_v,$$
$$F_p = Q_l = Q_r = F_{sLo} + F_{sUp} = F_s.$$

. As expected the flows through the lower compartments are equal and the overall flow is the same in the systemic, the pulmonary part, and the heart.

6.2 Derivation of equilibrium relations

To solve the ODE system with optimal control it is necessary to have the initial (steady) state and the final steady state. Our first approach was using the Mathematica function *FindRoot*, which uses a Newton method (which is a gradient routine) but got stuck rather often, because of the bad condition of the Jacobian ($\text{cond}(\nabla f) \approx 10^6$).

Since it is easier to debug Matlab programs compared to Mathematica programs, we recoded the model using the Matlab function *fsolve*, which seems to be a more robust scheme giving solutions in most cases. But a solution was not always found and the level of accuracy was unclear when found in some cases.

Thus it was useful to analyze the steady state equations analytically. Furthermore analysis is needed to investigate uniqueness of equilibrium points for a given parameter set.

In the model there are 19 variables, but we have only 17 ODEs, thus two states have to be picked to determine the steady state. We choose H, because it is easily accessible in experiments, and $P_{a_{CO_2}}$, because we assume that it is held rather constant at a level of 40 mmHg.

Our approach was to work separately with the cardiovascular and the respirator equations.

6.2.1 Solving the cardiovascular pressure equations (Eq. 2.1–2.5)

H and thus t_d are given. In Section 6.2.3 we derive S_l and S_r. We have thus the following steady state equations to examine:

From Equation (2.1):

$$\begin{aligned} 0 &= Q_l - F_a - F_{sUp} = Q_l - \frac{P_{asUp} - P_{asLo} + P_{grav}}{R_a} - \frac{P_{asUp} - P_{vsUp}}{R_s} \\ &= R_a R_s Q_l - (R_a + R_s) P_{asUp} + R_s P_{asLo} + R_a P_{vsUp} - R_s P_{grav}. \end{aligned}$$

From Equation (2.2):

$$\begin{aligned} 0 &= F_a - F_{sLo} = \frac{P_{asUp} - P_{asLo} + P_{grav}}{R_a} - \frac{P_{asLo} - P_{vsLo}}{R_s} \\ &= R_s P_{asUp} - (R_a + R_s) P_{asLo} + R_a P_{vsLo} + R_s P_{grav}. \end{aligned}$$

From Equation (2.3):

$$\begin{aligned} 0 = F_{sLo} - F_v &= \frac{P_{asLo} - P_{vsLo}}{R_s} - \frac{P_{vsLo} - P_{vsUp} - P_{grav}}{R_v} \\ &= R_v P_{asLo} - (R_v + R_s) P_{vsLo} + R_s P_{vsUp} + R_s P_{grav}. \end{aligned}$$

From Equation (2.4):

$$\begin{aligned} 0 = F_v - Q_r + F_{sUp} &= \frac{P_{vsLo} - P_{vsUp} - P_{grav}}{R_v} + \frac{P_{asUp} - P_{vsUp}}{R_s} - Q_r \\ &= R_v P_{asUp} + R_s P_{vsLo} - (R_v + R_s) P_{vsUp} - R_s P_{grav} - R_v R_s Q_r. \end{aligned}$$

From Equation (2.5):

$$\begin{aligned} 0 = F_p - Q_l &= \frac{P_{ap} - P_{vp}}{R_p} - Q_l \\ &= P_{ap} - P_{vp} - R_p Q_l. \end{aligned}$$

So we then have the following **five equations** to work with:

$$0 = R_a R_s Q_l(P_{vp}, P_{asUp}) - (R_a + R_s) P_{asUp} + R_s P_{asLo} + R_a P_{vsUp} - R_s P_{grav} \quad (6.1)$$

$$0 = R_s P_{asUp} - (R_a + R_s) P_{asLo} + R_a P_{vsLo} + R_s P_{grav} \quad (6.2)$$

$$0 = R_v P_{asLo} - (R_v + R_s) P_{vsLo} + R_s P_{vsUp} + R_s P_{grav} \quad (6.3)$$

$$0 = -R_v R_s Q_r(P_{ap}, P_{vsUp}) + R_v P_{asUp} + R_s P_{vsLo} - (R_v + R_s) P_{vsUp} - R_s P_{grav} \quad (6.4)$$

$$0 = P_{ap} - P_{vp} - R_p Q_l(P_{vp}, P_{asUp}). \quad (6.5)$$

From (**6.3**) dividing by R_v we derive a relation involving P_{asLo} :

$$\begin{aligned} P_{asLo} &= \frac{R_v + R_s}{R_v} P_{vsLo} - \frac{R_s}{R_v}(P_{vsUp} + P_{grav}) \\ &= \frac{R_v + R_s}{R_v} \frac{R_a + R_s}{R_a} P_{asLo} - \frac{R_v + R_s}{R_v} \frac{R_s}{R_a}(P_{asUp} + P_{grav}) - \frac{R_s}{R_v}(P_{vsUp} + P_{grav}) \end{aligned}$$

so that

$$P_{asLo}\left(\frac{R_v + R_s}{R_v}\frac{R_a + R_s}{R_a} - 1\right) = \frac{R_v + R_s}{R_v}\frac{R_s}{R_a} P_{asUp} + \frac{R_s}{R_v} P_{vsUp} + \frac{R_s}{R_v}\left(1 + \frac{R_v + R_s}{R_a}\right) P_{grav}.$$

From (**6.2**) dividing by R_a we derive P_{vsLo} :

$$0 = \frac{R_s}{R_a} P_{asUp} - \frac{R_a + R_s}{R_a} P_{asLo} + P_{vsLo} + \frac{R_s}{R_a} P_{grav}$$

implies

$$P_{vsLo} = \frac{R_a + R_s}{R_a} P_{asLo} - \frac{R_s}{R_a}(P_{asUp} + P_{grav}).$$

From (**6.5**) dividing by c_{ap} and adding Eq. (6.1) multiplied by $\frac{R_p}{R_a R_s}$ we derive the following relation involving P_{vp} :

$$\begin{aligned} 0 = &\frac{V_0}{c_{ap}} - \frac{c_{asUp}}{c_{ap}} P_{asUp} - \frac{c_{asLo}}{c_{ap}} P_{asLo} - \frac{c_{vsLo}}{c_{ap}} P_{vsLo} \\ &- \frac{c_{vsUp}}{c_{ap}} P_{vsUp} - \frac{c_{vp}}{c_{ap}} P_{vp} - P_{vp} - R_p Q_l \end{aligned}$$

implies

$$\left(1+\frac{c_{vp}}{c_{ap}}\right)P_{vp} = -\left(R_p\frac{R_a+R_s}{R_aR_s}+\frac{c_{asUp}}{c_{ap}}\right)P_{asUp}+\left(\frac{R_p}{R_a}-\frac{c_{asLo}}{c_{ap}}\right)P_{asLo} + \left(\frac{R_p}{R_s}-\frac{c_{vsUp}}{c_{ap}}\right)P_{vsUp}-\frac{c_{vsLo}}{c_{ap}}P_{vsLo}-\frac{R_p}{R_a}P_{grav}+\frac{V_0}{c_{ap}}.$$

Linear relations Thus the steady states of P_{asLo}, P_{vsLo} and P_{vp} can be related to the steady states of P_{asUp}, P_{vsUp}, P_{grav}, and to V_0 as follows. Using the above three relations involving P_{asLo}, P_{vsLo} and P_{vp} we have the following **linear relations**:

$$P_{asLo} = k_1P_{asUp}+k_2P_{vsUp}+k_3P_{grav} \tag{6.6}$$
$$P_{vsLo} = k_4P_{asUp}+k_5P_{vsUp}+k_6P_{grav} \tag{6.7}$$
$$P_{vp} = k_7P_{asUp}+k_8P_{vsUp}+k_9P_{grav}+k_{10}V_0, \tag{6.8}$$

where the following **parameters** are given to simplify the equation format:

$$\begin{array}{lllll}
k_1=\dfrac{R_v+R_s}{R_v+R_a+R_s} & \Rightarrow & 0<k_1<1 & \Rightarrow & -[R_a+R_s(1-k_1)]<0\\
k_2=\dfrac{R_a}{R_v+R_a+R_s} & \Rightarrow & 0<k_2<1 & & k_2=1-k_1\\
k_3=1 & \Rightarrow & k_3=1 & & \\
k_4=\dfrac{R_v}{R_v+R_a+R_s} & \Rightarrow & 0<k_4<1 & & \\
k_5=\dfrac{R_a+R_s}{R_v+R_a+R_s} & \Rightarrow & 0<k_5<1 & & k_5=1-k_4\\
k_6=1 & \Rightarrow & k_6=1 & & \\
k_7 \text{ see def. below} & \Rightarrow & k_7<0 & & \\
k_8 \text{ see def. below} & \Rightarrow & k_8\overset{?}{\approx}0 & & \\
k_9=-\dfrac{c_{asLo}+c_{vsLo}}{c_{ap}+c_{vp}} & \Rightarrow & k_9<0 & & \\
k_{10}=\dfrac{1}{c_{ap}+c_{vp}} & \Rightarrow & 1<k_{10} & & \\
k_k=\dfrac{1}{R_v+R_a+R_s} & \Rightarrow & 0<k_k<1 & & \\
k_s=\dfrac{R_s}{1+R_sk_k} & \Rightarrow & 1<k_s & & \\
k_l=\exp\left(-\dfrac{t_d}{R_lc_l}\right) & \Rightarrow & 0<k_l & & (0<t_d<1)\\
k_r=\exp\left(-\dfrac{t_d}{R_rc_r}\right) & \Rightarrow & 0<k_r. & &
\end{array}$$

Let us denote $P_l^{eff}=\min(S_l,P_{asUp})$ $P_r^{eff}=\min(S_r,P_{ap})$.
Next, setting $Q_l=\frac{k_{11}P_{vp}}{P_{asUp}+k_{12}}$, $Q_r=\frac{k_{13}P_{vsUp}}{P_{ap}+k_{14}}$, we have the following relations:

$$k_{11}=Hc_lP_l^{eff} \quad\Rightarrow\quad 0<k_{11} \qquad k_{13}=Hc_rP_r^{eff} \quad\Rightarrow\quad 0<k_{13}$$
$$k_{12}=P_l^{eff}\frac{k_l}{1-k_l} \quad\Rightarrow\quad 0<k_{12} \qquad k_{14}=P_r^{eff}\frac{k_r}{1-k_r} \quad\Rightarrow\quad 0<k_{14}$$

.

Finally we give k_7 and k_8 :

$$\begin{aligned}
k_7 &= \left(1+\frac{c_{vp}}{c_{ap}}\right)^{-1} * \left[-\left(R_p\frac{R_a+R_s}{R_aR_s}+\frac{c_{asUp}}{c_{ap}}\right)\right.\\
&\quad \left.+\left(\frac{R_p}{R_a}-\frac{c_{asLo}}{c_{ap}}\right)\frac{R_v+R_s}{R_v+R_a+R_s}-\frac{c_{vsLo}}{c_{ap}}\frac{R_v}{R_v+R_a+R_s}\right]\\
&= \left(\frac{c_{ap}}{c_{ap}+c_{vp}}\right) * \left[-\left(R_pc_{ap}\frac{R_a+R_s}{R_aR_sc_{ap}}+\frac{R_ac_{asUp}}{R_ac_{ap}}\right)\right.\\
&\quad \left.+\left(\frac{R_pc_{ap}}{R_ac_{ap}}-\frac{R_ac_{asLo}}{R_ac_{ap}}\right)\frac{R_v+R_s}{R_v+R_a+R_s}-\frac{R_ac_{vsLo}}{R_ac_{ap}}\frac{R_v}{R_v+R_a+R_s}\right]\\
&= \left(\frac{1}{R_aR_s(c_{ap}+c_{vp})}\right) * [-R_p(R_a+R_s)c_{ap}-R_aR_sc_{asUp}\\
&\quad +(R_pR_sc_{ap}-R_aR_sc_{asLo})\frac{R_v+R_s}{R_v+R_a+R_s}-\frac{R_vR_aR_s}{R_v+R_a+R_s}c_{vsLo}\Big]\\
&= \left(\frac{1}{R_aR_s(c_{ap}+c_{vp})}\right) * [-R_p(R_a+k_2R_s)c_{ap}-R_aR_sc_{asUp}-k_2R_s(R_v+R_s)c_{asLo}-k_2R_vR_sc_{vsLo}]\\
&= -\frac{1}{c_{ap}+c_{vp}}\left[R_p(\frac{1}{R_s}+k_k)c_{ap}+c_{asUp}+k_1c_{asLo}+k_4c_{vsLo}\right].
\end{aligned}$$

and

$$\begin{aligned}
k_8 &= \left(1+\frac{c_{vp}}{c_{ap}}\right)^{-1} * \left[\left(\frac{R_p}{R_s}-\frac{c_{vsUp}}{c_{ap}}\right)\right.\\
&\quad \left.+\left(\frac{R_p}{R_a}-\frac{c_{asLo}}{c_{ap}}\right)\frac{R_a}{R_v+R_a+R_s}-\frac{c_{vsLo}}{c_{ap}}\frac{R_a+R_s}{R_v+R_a+R_s}\right]\\
&= \left(\frac{1}{R_aR_s(c_{ap}+c_{vp})}\right) * [R_pR_ac_{ap}-R_aR_sc_{vsUp}\\
&\quad +(R_pR_sc_{ap}-R_aR_sc_{asLo})\frac{R_a}{R_v+R_a+R_s}-R_aR_sc_{vsLo}\frac{R_a+R_s}{R_v+R_a+R_s}\Big]\\
&= \frac{1}{c_{ap}+c_{vp}}\left[R_p(\frac{1}{R_s}+k_k)c_{ap}-c_{vsUp}-k_2c_{asLo}-k_5c_{vsLo}\right].
\end{aligned}$$

From (**6.1**) we derive P_{vsUp} in terms of P_{asUp} :

$$\begin{aligned}
0 &= -(R_a+R_s)P_{asUp}+R_sP_{asLo}+R_aP_{vsUp}-R_sP_{grav}+R_aR_sQ_l(P_{vp},P_{asUp})\\
&= -(R_a+R_s(1-k_1))P_{asUp}+(R_a+R_sk_2)P_{vsUp}-R_s(1-k_3)P_{grav}+R_aR_sk_{11}\frac{P_{vp}}{P_{asUp}+k_{12}}\\
&= -(R_a+R_s(1-k_1))P_{asUp}+(R_a+R_sk_2)P_{vsUp}+R_aR_sk_{11}\frac{P_{vp}}{P_{asUp}+k_{12}}\\
&= [P_{asUp}+k_{12}][-(R_a+R_sk_2)P_{asUp}+(R_a+R_sk_2)P_{vsUp}]\\
&\quad +R_aR_sk_{11}(k_7P_{asUp}+k_8P_{vsUp}+k_9P_{grav}+k_{10}V_0).
\end{aligned}$$

implies

$$\begin{aligned}
P_{vsUp} &= -\frac{[R_aR_sk_7k_{11}-(P_{asUp}+k_{12})(R_a+R_sk_2)]P_{asUp}+R_aR_sk_{11}(k_9P_{grav}+k_{10}V_0)}{(P_{asUp}+k_{12})(R_a+R_sk_2)+R_aR_sk_8k_{11}}\\
&= \frac{P_{asUp}^2+(k_{12}-k_sk_7k_{11})P_{asUp}-k_sk_{11}(k_9P_{grav}+k_{10}V_0)}{P_{asUp}+k_{12}+k_sk_8k_{11}}.
\end{aligned}$$

where $k_s = \frac{R_s}{1+R_s k_k}$ is introduced for simplification of format. Introducing constants b_1, b_2, and b_3 defined in the obvious way to simplify the format we see that

$$P_{vsUp} = \frac{P_{asUp}^2 + b_1 P_{asUp} - b_2}{P_{asUp} + b_3}. \tag{6.9}$$

From (**6.4**) we derive a relation involving P_{asUp} :

$$\begin{aligned}
0 &= -R_v R_s Q_r(P_{ap}, P_{vsUp}) + R_v P_{asUp} + R_s P_{vsLo} - (R_v + R_s) P_{vsUp} - R_s P_{grav} \\
&= -R_v R_s k_{13} \frac{P_{vsUp}}{P_{ap} + k_{14}} + (R_v + R_s k_4) P_{asUp} - (R_v + R_s - R_s k_5) P_{vsUp} - R_s (1 - k_6) P_{grav} \\
&= R_v R_s k_{13} \frac{P_{vsUp}}{P_{ap} + k_{14}} - (R_v + R_s k_4) P_{asUp} + (R_v + R_s k_4) P_{vsUp} \\
&= R_v R_s k_{13} P_{vsUp} - k_{14}(R_v + R_s k_4)(P_{asUp} - P_{vsUp}) \\
&\quad - \frac{1}{c_{ap}} [V_0 - c_{asUp} P_{asUp} - c_{asLo} P_{asLo} - c_{vsLo} P_{vsLo} - c_{vsUp} P_{vsUp} - c_{vp} P_{vp}] \\
&\quad * (R_v + R_s k_4)(P_{asUp} - P_{vsUp}) \\
&= R_v R_s k_{13} P_{vsUp} - k_{14}(R_v + R_s k_4)(P_{asUp} - P_{vsUp}) \\
&\quad - \frac{1}{c_{ap}} [V_0 - c_{asUp} P_{asUp} - c_{vsUp} P_{vsUp} \\
&\quad - (k_1 c_{asLo} + k_4 c_{vsLo} + k_7 c_{vp}) P_{asUp} - (k_2 c_{asLo} + k_5 c_{vsLo} + k_8 c_{vp}) P_{vsUp} \\
&\quad - (k_3 c_{asLo} + k_6 c_{vsLo} + k_9 c_{vp}) P_{grav} - k_{10} V_0] * (R_v + R_s k_4)(P_{asUp} - P_{vsUp}) \\
&= \frac{c_{ap} k_s k_{13}}{(P_{asUp} - P_{vsUp})} P_{vsUp} \\
&\quad + (c_{asUp} + k_1 c_{asLo} + k_4 c_{vsLo} + k_7 c_{vp}) P_{asUp} \\
&\quad + (c_{vsUp} + k_2 c_{asLo} + k_5 c_{vsLo} + k_8 c_{vp}) P_{vsUp} \\
&\quad + (c_{asLo} + c_{vsLo} + k_9 c_{vp}) P_{grav} - c_{ap} k_{14} + (k_{10} - 1) V_0
\end{aligned}$$

substituting the relation (6.9) for P_{vsUp} we have:

$$\begin{aligned}
0 &= a_1 \frac{P_{vsUp}}{P_{asUp} - P_{vsUp}} + a_2 P_{asUp} + a_3 P_{vsUp} + a_4 \\
0 &= a_1 \frac{P_{asUp}^2 + b_1 P_{asUp} - b_2}{P_{asUp}(P_{asUp} + b_3) - P_{asUp}^2 + b_1 P_{asUp} - b_2} + a_2 P_{asUp} + a_3 \frac{P_{asUp}^2 + b_1 P_{asUp} - b_2}{P_{asUp} + b_3} + a_4 \\
0 &= a_1 \frac{P_{asUp}^2 + b_1 P_{asUp} - b_2}{(b_1 + b_3) P_{asUp} - b_2} + \frac{(a_2 + a_3) P_{asUp}^2 + (a_2 b_3 + b_1 + a_4) P_{asUp} + (a_4 b_3 - b_2)}{P_{asUp} + b_3} \\
0 &= a_1 P_{asUp}^3 + a_1 (b_1 + b_3) P_{asUp}^2 + a_1 (b_1 b_3 - b_2) P_{asUp} - a_1 b_2 b_3 \\
&\quad + (b_1 + b_3)(a_2 + a_3) P_{asUp}^3 + [(a_2 b_3 + b_1 + a_4)(b_1 + b_3) - (a_2 + a_3) b_2] P_{asUp}^2 \\
&\quad + [(a_4 b_3 - b_2)(b_1 + b_3) - b_2 (a_2 b_3 + b_1 + a_4) P_{asUp} - b_2 (a_4 b_3 - b_2)
\end{aligned}$$

This leads to:

$$\begin{aligned}
0 &= [a_1 + (b_1 + b_3)(a_2 + a_3)] P_{asUp}^3 + [(a_1 + a_2 b_3 + b_1 + a_4)(b_1 + b_3) - (a_2 + a_3) b_2] P_{asUp}^2 \\
&\quad + [a_1 (b_1 b_3 - b_2) + (a_4 b_3 - b_2)(b_1 + b_3) - b_2 (a_2 b_3 + b_1 + a_4)] P_{asUp} \\
&\quad - [b_2 (a_1 b_3 + a_4 b_3 - b_2)].
\end{aligned} \tag{6.10}$$

We thus derive the expression 6.10 for P_{asUp} involving a cubic equation, which may have either one real and two imaginary or three real solutions.

6.2.2 Solving the respiratory equations (Eq. 2.6–2.10)

Plugging (**2.9**) divided by F_s into (**2.6**) we derive $P_{a_{CO_2}}$:

$$\begin{aligned} 0 &= \frac{863 F_p M R_{CO_2}}{F_s} + \dot{V}_A \left(P_{I_{CO_2}} - P_{a_{CO_2}} \right) \\ \Rightarrow P_{a_{CO_2}} &= \frac{863 F_p M R_{CO_2}}{F_s \dot{V}_A} + P_{I_{CO_2}}. \end{aligned} \tag{6.11}$$

Plugging (**2.10**) divided by F_s into (**2.7**) we derive $P_{a_{O_2}}$:

$$\begin{aligned} 0 &= -\frac{863 F_p M R_{O_2}}{F_s} + \dot{V}_A \left(P_{I_{O_2}} - P_{a_{O_2}} \right) \\ \Rightarrow P_{a_{O_2}} &= -\frac{863 F_p M R_{O_2}}{F_s \dot{V}_A} + P_{I_{O_2}}. \end{aligned} \tag{6.12}$$

From (**2.8**) we derive $C_{B_{CO_2}}$:

$$C_{B_{CO_2}} = \frac{M R_{B_{CO_2}}}{F_B} + C_{a_{CO_2}}. \tag{6.13}$$

From (**2.9**) we derive $C_{v_{CO_2}}$:

$$C_{v_{CO_2}} = \frac{M R_{CO_2}}{F_s} + C_{a_{CO_2}}. \tag{6.14}$$

From (**2.10**) we derive $C_{v_{O_2}}$:

$$C_{v_{O_2}} = -\frac{M R_{O_2}}{F_s} + C_{a_{O_2}}. \tag{6.15}$$

6.2.3 Solving stroke volume and control equations (Eq. 2.11–2.17)

$$\sigma_l = 0 \tag{6.16}$$

$$\sigma_r = 0 \tag{6.17}$$

$$S_l = \frac{\beta_l}{\alpha_l} H \tag{6.18}$$

$$S_r = \frac{\beta_r}{\alpha_r} H \tag{6.19}$$

$$u_i = 0 \qquad i = 1, 2, 3 \tag{6.20}$$

6.2.4 Conclusion

From these calculations we see that all cardiovascular steady states can be solved for in terms of P_{asUp} while all respiratory steady states can be written in terms of $P_{v_{O_2}}$ (or equivalently $C_{v_{O_2}}$). Furthermore, P_{asUp} and $P_{v_{O_2}}$ are interdependent. $P_{v_{O_2}}$ depends on F_s which depends on P_{asUp} while P_{asUp} depends on R_s which depends on $C_{v_{O_2}}$ and thus $P_{v_{O_2}}$. Simultaneously solving the equations Eq. 6.10 and Eq. 6.15 for P_{asUp} and $P_{v_{O_2}}$ will provide the steady state solutions for any parameter set. To implement an efficient algorithm for finding equilibriums and testing these equilibriums for uniqueness, we implement an algorithm presented in the next section.

6.3 Program algorithm

For calculation of the steady state we use the Matlab function *fsolve*. Given the above derived dependencies it is only necessary to search for values of P_{asUp} and $P_{v_{O_2}}$ to derive the other state variables. Thus we proceed by minimizing the deviation from zero of the system steady state equations based on searching candidate values of P_{asUp} and $P_{v_{O_2}}$. This scheme is equivalent to applying *fsolve* to the full system but is more efficient and stable.

For the cardiovascular part of the scheme we have to distinguish between the cases $S_l < P_{asUp}$ and $S_l \geq P_{asUp}$. This is easy to do as S_l can be easily calculated according to Section 6.2.3 and P_{asUp} is given.

Thus using $P^{eff} = \min(S_l, P_{asUp})$ we find P_{vsUp}:

$$P_{vsUp} = \frac{P_{asUp}^2 + P^{eff}(k_{12} - k_s k_7 k_{11})P_{asUp} - P^{eff} k_s k_{11}(k_9 P_{grav} + k_{10} V_0)}{P_{asUp} + P^{eff} k_{12} + P^{eff} k_s k_8 k_{11}}$$

where

$$\begin{aligned} k_s &= \frac{R_s}{1 + R_s k_k} \\ k_{11} &= c_l * H \\ k_{12} &= \frac{k_l}{1 - k_l}. \end{aligned}$$

We can then calculate

$$\begin{aligned} P_{asLo} &= k_1 P_{asUp} + (1 - k_1) P_{vsUp} + P_{grav} \\ P_{vsLo} &= k_4 P_{asUp} + (1 - k_4) P_{vsUp} + P_{grav} \\ P_{vp} &= k_7 P_{asUp} + k_8 P_{vsUp} + k_9 P_{grav} + k_{10} V_0 \end{aligned}$$

where

$$\begin{aligned} k_1 &= \frac{R_v + R_s}{R_v + R_a + R_s} \\ k_4 &= \frac{R_v}{R_v + R_a + R_s} \\ k_7 &= -\frac{1}{c_{ap} + c_{vp}} \left(R_p(\frac{1}{R_s} + k_k) c_{ap} + c_{asUp} + k_1 c_{asLo} + k_4 c_{vsLo} \right) \\ k_8 &= \frac{1}{c_{ap} + c_{vp}} \left(R_p(\frac{1}{R_s} + k_k) c_{ap} - c_{vsUp} - (1 - k_1) c_{asLo} - (1 - k_4) c_{vsLo} \right) \\ k_9 &= -\frac{c_{asLo} + c_{vsLo}}{c_{ap} + c_{vp}} \\ k_{10} &= \frac{1}{c_{ap} + c_{vp}}. \end{aligned}$$

Additionally using the solutions of Section 6.2.2 we get the respiratory states and then can calculate the deviations of the steay state equations mentioned above.

Note This algorithm solves the steady states with exact maximum and minimum functions, whereas the original implemented ODEs used smoothed max and min functions and as a result we always have some small deviation between the calculated steady states in the two formulation.

7 Results

For comparison of simulations of the full model proposed in this report, we performed HUT experiments measuring several quantities.

7.1 Data measurements

Fig. 11 shows a set of data measured at a HUT from 0^o to 70^o in 10 sec with Finapres^{TM} from a 25 year old male human.

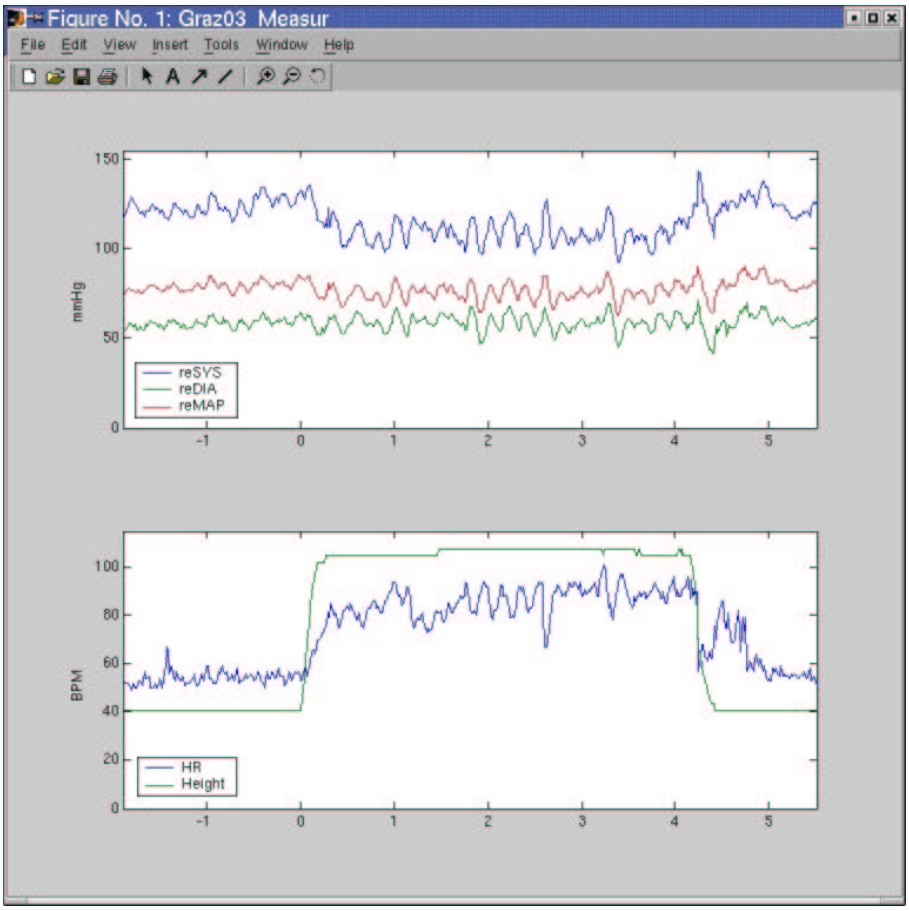

Figure 11: Measurement of 70^o tilt in 10 sec.

7.2 Fitting the data

In Fig. 12 we show the results of a parameter fit, which was done by first adjusting some model parameters to fit the steady state and afterwards adjusting the weights in the cost functional to fit the dynamics. (Steady state values and parameters in Appendix B)

The volume shift of blood into the venous leg compartment was 800 ml.

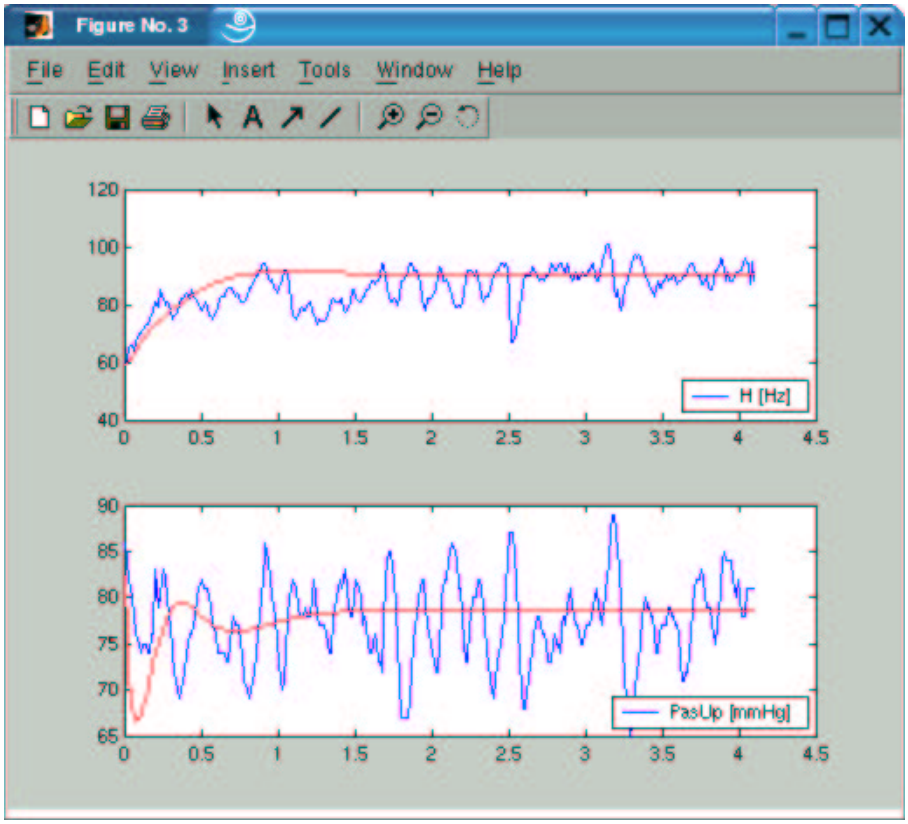

Figure 12: This is the model fitting the data

Fitting steady states

The variable TiltingAngle went from 0 to 70 degrees in 10 sec, heart rate went up from 59 to 90.6 and c_{vsLo} and A_{pesk} were set to match the Pas_{up} steady state ($c_{vsLo} = 0.7*(1-frac)*(0.75 \rightarrow 0.115)$ and $A_{pesk} = 131.61*(0.95 \rightarrow 1.08)$). Rather important is also the fact, that we had to adjust the fraction of upper and lower compartments to $frac = 0.3$ to get reasonable results.

Fitting dynamics

To fit the dynamics we adjust the weights in the cost function for the optimal control. There are two different weight-vectors: $WeightsU$ and $WeightsX$.

WeightsU puts weights on changes of the control

WeightsX puts weights on deviations from the final steady state

The fit was done by estimating the weights for the control. We used all three control weights and weights for Pas_{up} and H, $P_{a_C O_2}$ and $P_{a_{O_2}}$.

For this data set, the weights necessary to fit the data indicate a strong influence of the cardio-pulmonary control loop.

7.3 Ongoing work

The model exhibits reasonable performance as compared against data. The next steps are anticipated in terms of model development.

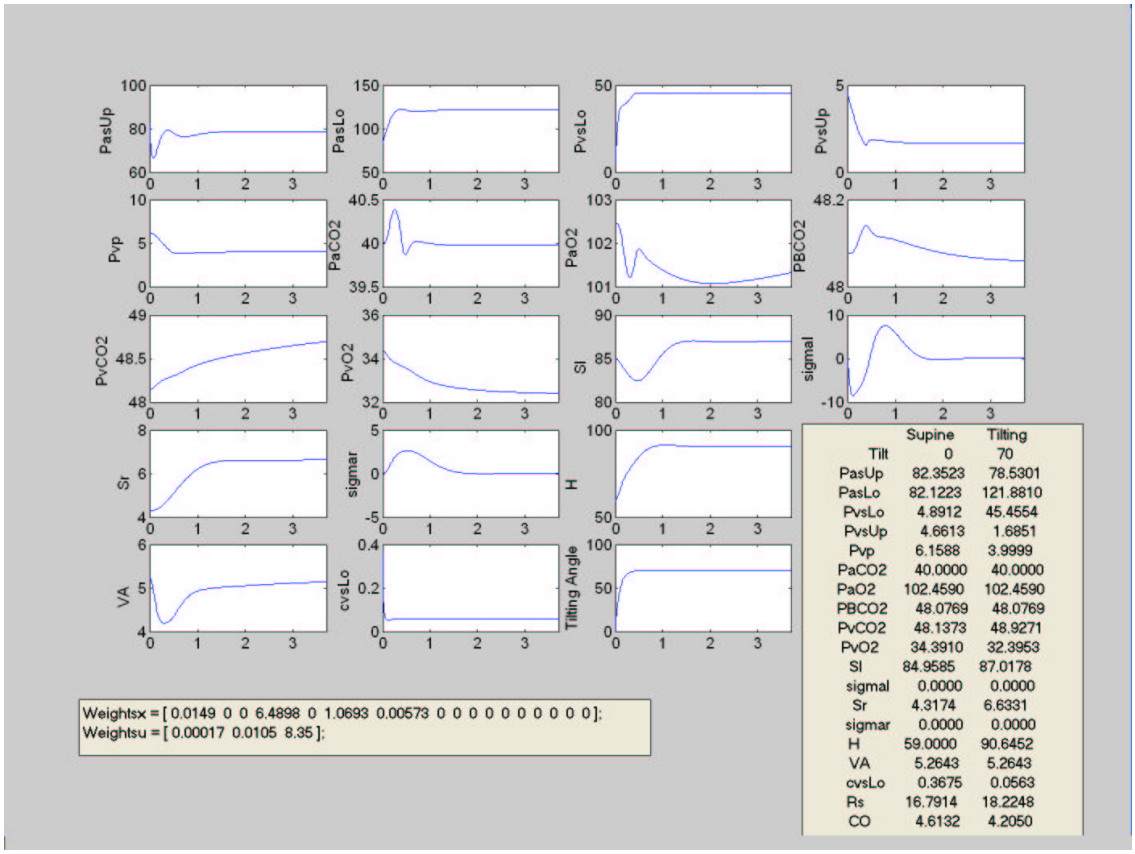

	Supine	Tilting
Tilt	0	70
PasUp	82.3523	78.5301
PasLo	82.1223	121.8810
PvsLo	4.8912	45.4554
PvsUp	4.6613	1.6851
Pvp	6.1588	3.9999
PaCO2	40.0000	40.0000
PaO2	102.4590	102.4590
PBCO2	48.0769	48.0769
PvCO2	48.1373	48.9271
PvO2	34.3910	32.3953
SI	84.9585	87.0178
sigmal	0.0000	0.0000
Sr	4.3174	6.6331
sigmar	0.0000	0.0000
H	59.0000	90.6452
VA	5.2643	5.2643
cvsLo	0.3675	0.0563
Rs	16.7914	18.2248
CO	4.6132	4.2050

Figure 13: Complete model output for the fitted data

- Analytical studies
  1. The analytical results on steady state analysis will be further developed
  2. Analytical results on the two dimensional model comparisons between LBNP and HUT will be done to clarify the degree to which the two orthostatic stress models are different, when they can be used interchangeably, and when they must be distinguished.
- Physiological modeling
  1. Further experimental data will be collected and analyzed. As well as parameter identification performed with test subjects.
  2. There are physiological differences between fast and slow tilt, as well as between small and large tilt. In small tilt low pressure sensors play a more prominent role and implementation of this control loop effect needs to be studied. Fast tilt involves buffering by the lung blood volume and this needs to be studied as well.
  3. Implementation of sympathetic effect on contractility should be explored as a control, currently implemented as a parameter change.
  4. The baroreceptors in the carotid artery are situated above the heart and sense a slightly different pressure from the aortic sensors (which measure P_{asUp}). The effects of this variation in pressure are not modeled.

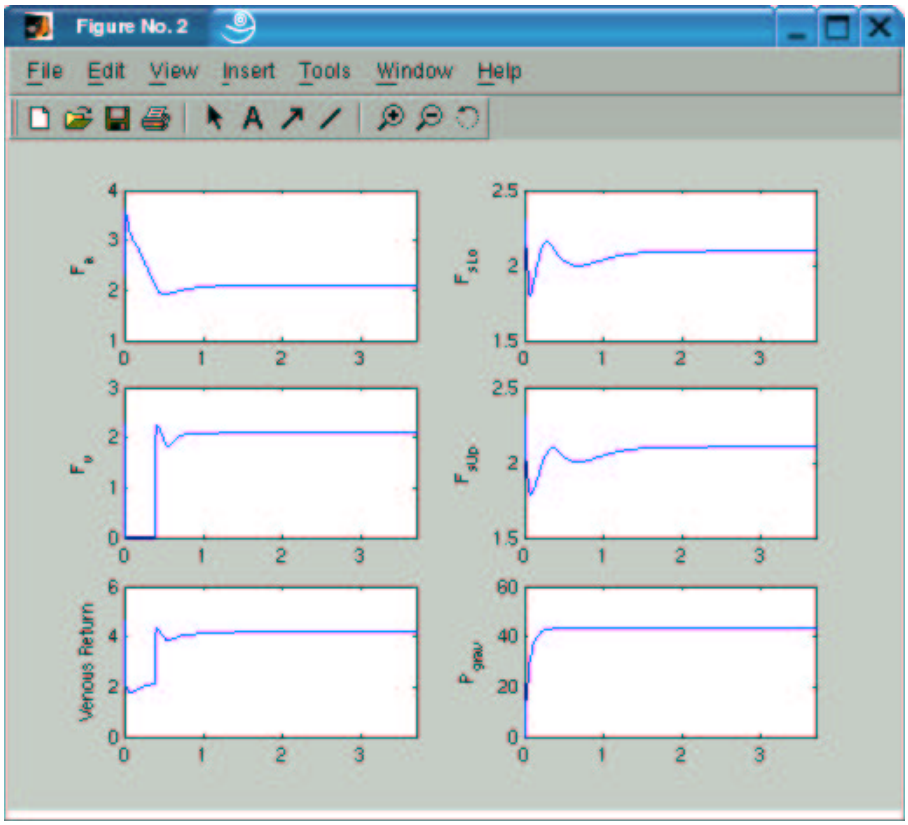

Figure 14: Flows between the systemic compartments for the fitted data

A Symbol definitions

Respiratory parameters

Symbol	Meaning	unit
MR_{CO_2}	metabolic CO_2 production rate	$\mathrm{l_{STPD}} \cdot \mathrm{min}^{-1}$
MR_{O_2}	metabolic O_2 consumption rate	$\mathrm{l_{STPD}} \cdot \mathrm{min}^{-1}$
$C_{a_{CO_2}}$	concentration of CO_2 in arterial blood	mmHg
$C_{a_{O_2}}$	concentration of O_2 in arterial blood	mmHg
$P_{a_{CO_2}}$	partial pressure of CO_2 in arterial blood	mmHg
$P_{a_{O_2}}$	partial pressure of O_2 in arterial blood	mmHg
$P_{v_{CO_2}}$	partial pressure of CO_2 in mixed venous blood	mmHg
$P_{v_{O_2}}$	partial pressure of O_2 in mixed venous blood	mmHg
$\dot{V}_A$	alveolar ventilation	$\mathrm{l_{BTPS}} \cdot \mathrm{min}^{-1}$
$V_{A_{CO_2}}$	effective CO_2 storage volume of the lung compartment	$\mathrm{l_{BTPS}}$
$V_{A_{O_2}}$	effective O_2 storage volume of the lung compartment	$\mathrm{l_{BTPS}}$
$V_{T_{CO_2}}$	effective tissue storage volume for CO_2	l
$V_{T_{O_2}}$	effective tissue storage volume for O_2	l
$V_{B_{CO_2}}$	effective tissue storage volume for O_2	l
K, k, m	dissociation constants relating concen.to partial pressure	
G_c	central controller gain factor	$\mathrm{l}/(\mathrm{min} \cdot \mathrm{mmHg})$
G_p	peripheral controller gain factor	$\mathrm{l}/(\mathrm{min} \cdot \mathrm{mmHg})$
I_c	central drive threshold value	mmHg
I_p	peripheral drive threshold value	mmHg

Cardiovascular parameters

Symbol	Meaning	Unit
α_l	coefficient of S_l in the differential equation for σ_l	min^{-2}
α_r	coefficient of S_r in the differential equation for σ_r	min^{-2}
A_{pesk}	$R_s = A_{\mathrm{pesk}} C_{v_{O_2}}$	$\mathrm{mmHg} \cdot \mathrm{min} \cdot \mathrm{l}^{-1}$
β_l	coefficient of H in the differential equation for σ_l	$\mathrm{mmHg} \cdot \mathrm{min}^{-1}$
β_r	coefficient of H in the differential equation for σ_r	$\mathrm{mmHg} \cdot \mathrm{min}^{-1}$
$frac$	upper compartment fraction of basic prone capacitance	l
c_{as}	compliance of the arterial part of the systemic circuit	$\mathrm{l} \cdot \mathrm{mmHg}^{-1}$
c_{ap}	compliance of the arterial part of the pulmonary circuit	$\mathrm{l} \cdot \mathrm{mmHg}^{-1}$
c_{vs}	compliance of the venous part of the systemic circuit	$\mathrm{l} \cdot \mathrm{mmHg}^{-1}$
c_{vp}	compliance of the venous part of the pulmonary circuit	$\mathrm{l} \cdot \mathrm{mmHg}^{-1}$
F_p	blood flow perfusing the lung compartment	$\mathrm{l} \cdot \mathrm{min}^{-1}$
F_s	blood flow perfusing the tissue compartment	$\mathrm{l} \cdot \mathrm{min}^{-1}$
H	heart rate	min^{-1}
γ_l	coefficient of σ_l in the differential equation for σ_l	min^{-1}
γ_r	coefficient of σ_r in the differential equation for σ_r	min^{-1}
P_{as}	mean blood pressure in arterial region: systemic circuit	mmHg
P_{ap}	mean blood pressure in arterial region: pulmonary circuit	mmHg
P_{vs}	mean blood pressure in venous region: systemic circuit	mmHg
P_{vp}	mean blood pressure in venous region: pulmonary circuit	mmHg
Q_l	left cardiac output	$\mathrm{l} \cdot \mathrm{min}^{-1}$
Q_r	right cardiac output	$\mathrm{l} \cdot \mathrm{min}^{-1}$
R_p	resistance in the peripheral region of the pulmonary circuit	$\mathrm{mmHg} \cdot \mathrm{min} \cdot \mathrm{l}^{-1}$
R_s	peripheral resistance in the systemic circuit	$\mathrm{mmHg} \cdot \mathrm{min} \cdot \mathrm{l}^{-1}$
S	contractility of the ventricle	mmHg
σ	derivative of S	$\mathrm{mmHg} \cdot \mathrm{min}^{-1}$
u	control function	
V_{str}	stroke volume of the ventricle	l
V_0	total blood volume	l
$l,\ \ r$	left, right heart circuit respectively	

B Values for the data fit

Steady state values

State variable	Supine	Tilt
Tilting Angle	0	70
P_{asUp}	82.35	78.53
P_{asLo}	82.12	121.88
P_{vsLo}	4.89	45.45
P_{vsUp}	4.66	1.69
P_{vp}	6.16	4.00
$P_{a_{CO_2}}$	40.00	40.00
$P_{a_{O_2}}$	102.46	102.46
$P_{B_{CO_2}}$	48.08	48.08
$P_{v_{CO_2}}$	48.14	48.08
$P_{v_{O_2}}$	34.39	32.39
S_l	84.96	87.02
S_r	4.32	6.63
σ_l	0.00	0.00
σ_r	0.00	0.00
H	59.00	90.65
$\dot{V}_A$	5.26	5.26
c_{vsLo}	0.368	0.056
R_s	16.79	18.22
A_{pesk}	124.60	141.65
β_l	128.83	85.89
Q	4.61	4.21

Weights for Riccati

State variable	WeightsX
P_{asUp}	0.015
P_{asLo}	0
P_{vsLo}	0
P_{vsUp}	6.49
P_{vp}	0
$P_{a_{CO_2}}$	1.07
$P_{a_{O_2}}$	0.006
$P_{B_{CO_2}}$	0
$P_{v_{CO_2}}$	0
$P_{v_{O_2}}$	0
S_l	0
S_r	0
σ_l	0
σ_r	0
H	0
$\dot{V}_A$	0
c_{vsLo}	0

Control variable	WeightsU
u_1	0.0002
u_2	0.0105
u_3	8.3500

Parameter values

Parameters were either taken from [Tim98] or fitted*. R_a and R_v were chosen as small as reasonable.

Parameter	Value
V	5.0
frac	0.3
c_{asUp}	0.01002*frac
c_{asLo}	0.01002*(1-frac)
c_{vsUp}	0.70*frac
c_{vsLo}	State dependent
c_{ap}	0.03557
c_{vp}	0.1394
A_{pesk}	State dependent
MR_{O_2}	0.290
MR_{CO_2}	0.244
$MRBCO2$	0.042
F_B	0.800
α_l	89.47
α_r	28.46
β_l	State dependent
β_r	2.08
γ_l	37.33
γ_r	11.88
c_l	0.01289
c_r	0.06077
$K1$	0.2
$K2$	0.05
$kCO2$	0.244
$KCO2$	0.0065
$P_{I_{CO_2}}$	0.0
$P_{I_{O2}}$	150.0
R_l	11.35
R_r	4.158
R_a	0.1
R_v	0.1
$V_{B_{CO_2}}$	0.900
V_{CO_2}	3.200
V_{O_2}	2.500
$V_{T_{CO_2}}$	15.000
$V_{T_{O_2}}$	6.000

For units refer to the previous section.

List of Figures

References

[Ber97] Berne R, Levy M. *Cardiovascular physiology*. Mosby, St.Louis, 7th edition, 1997.

[Boy72] Boyers DG, Cuthbertson JG, Luetscher JA. Simulation of the human cardiovascular system: a model with normal response to change in posture, blood loss, transfusion, and autonomic blockade. *Simulation*, 18:197–205, 1972.

[Bur00] Burton RR. Mathematical models for predicting g-duration tolerances. *Aviat Space Env Med*, 71:981–90, 2000.

[Cro74] Croston RC, Fitzjerrell DG. Cardiovascular model for the simulation of exercise, lower body negative pressure, and tilt table experiments. In *Proc 5th Ann Pittsburgh Conf Modeling Simulation*, pages 471–6, 1974.

[Hao03] Hao WY, Bai J, Wu XY, Zhang LF. Simulation study of the effects of hypovolaemia on cardiovascular response to orthostatic stress. *Med Biol Eng Comput*, 41(1):44–51, 2003.

[Hel02] Heldt T, Shim EB, Kamm RD, Mark RG. Computational modeling of cardiovascular response to orthostatic stress. *J Appl Physiol*, 92:1239–54, 2002.

[Kap93] Kappel F, Peer RO. A mathematical model for fundamental regulation processes in the cardiovascular system. *J Math Biol*, 31(6):611–31, 1993.

[Kar94] Karam EH, Srinivasan RS, Charles JB, Fortney SM. The effect of blood volume loss on cardiovascular response to lower body negative pressure using a mathematical model. *J Gravit Physiol*, 1(1):P96–7, 1994.

[Leo79] Leonard JI, Leach CS, Rummel JA. Computer simulations of postural change, water immersion, and bedrest: an integrative approach for understanding the spaceflight response. *Physiologist*, 22:S31–2, 1979.

[Mel92] Melchior FM, Srinivasan RS, Clerè JM. Mathematical modeling of the human response to LBNP. *Physiologist*, 35:S204–5, 1992.

[Mel94] Melchior FM, Srinivasan RS, Thullier PH, Clerè JM. Simulation of cardiovascular response to lower body negative pressure from 0 mmHg to 40 mmHg. *J Appl Physiol*, 77:630–40, 1994.

[Pat89] Patton HD, Fuchs AF, Hille B, Scher AM, Steiner R, editor. *Textbook of physiology*. W.B. Saunders Company, Philadelphia, 1989.

[Pet01] Peterson K, Sharp MK, Pantalos GM. Simulation of the effects of gravity and posture on cardiovascular function. In *Bioengineering Conference*, volume 50, pages 897–8. ASME, 2001.

[Pet02] Peterson K, Ozawa ET, Pantalos GM, Sharp MK. Numerical simulation of the influence of gravity and posture on cardiac performance. *Ann Biomed Eng*, 30(2):247–59, 2002.

[Row86] Rowell LB. Adjustments to upright posture and blood loss. In *Human circulation regulation during physical stress*, pages 137–73. Oxford University Press, N.Y., 1986.

[Row93] Rowell LB. *Human cardiovascular control*. Oxford University Press, 1993.

[Rus79] Russell RD. *Mathematics of finite-dimensional control systems: theory and design*. Marcel Dekker, N.Y., 1979.

[Ste01] Stewart JM, Lavin J, Weldon A. Orthostasis fails to produce active limb venoconstriction in adolescents. *J Appl Physiol*, 91:1723–9, 2001.

[Sud93] Sud VK, Srinivasan R, Charles JB, Bungo MW. Effects of lower body negative pressure on blood flow with applications to the human cardiovascular system. *Med Biol Eng Comput*, 31:569–75, 1993.

[Tim98] Timischl S. *A global model of the cardiovascular and respiratory system*. PhD thesis, Karl Franzens Universität Graz, Austria, 1998.

[Wal01] Walsh C, Cirovic S, Frase WD, Samin A. A model of short term cardiovascular regulation. In *Bioengineering Conference*, volume 50, pages 901–2. ASME, 2001.

[Whi83] White RJ, Fitzjerrell DG, Croston RC. *Fundamentals of lumped compartmental modelling of the cardiovascular system*, volume 5.1, pages 162–84. Karger, Basel, 1983.